JOURNAL OF GEOPHYSICAL RESEARCH, VOL. 102, NO. D5, PAGES 5953–5970, MARCH 20, 1997

Evaluation and intercomparison of global atmospheric transport models using ^{222}Rn and other short-lived tracers

Daniel J. Jacob,[1] Michael J. Prather,[2] Philip J. Rasch,[3] Run-Lie Shia,[4] Yves J. Balkanski,[5] Stephen R. Beagley,[6] Daniel J. Bergmann,[7] W.T. Blackshear,[8] Margaret Brown,[9,10] Masaru Chiba,[11] Martyn P. Chipperfield,[12] J. de Grandpré,[6] Jane E. Dignon,[7] Johann Feichter,[13] Christophe Genthon,[14] W.L. Grose,[8] Prasad S. Kasibhatla,[15] Ines Köhler,[16] Mark A. Kritz,[17] Kathy Law,[12] Joyce E. Penner,[7] Michel Ramonet,[18] Claire E. Reeves,[19] Douglas A. Rotman,[7] Deianeira Z. Stockwell,[12] Peter F.J. Van Velthoven,[20] Gé Verver,[20] Oliver Wild,[12] Hu Yang,[9] Peter Zimmermann[21]

Abstract. Simulations of ^{222}Rn and other short-lived tracers are used to evaluate and intercompare the representations of convective and synoptic processes in 20 global atmospheric transport models. Results show that most established three-dimensional models simulate vertical mixing in the troposphere to within the constraints offered by the observed mean ^{222}Rn concentrations and that subgrid parameterization of convection is essential for this purpose. However, none of the models captures the observed variability of ^{222}Rn concentrations in the upper troposphere, and none reproduces the high ^{222}Rn concentrations measured at 200 hPa over Hawaii. The established three-dimensional models reproduce the frequency and magnitude of high-^{222}Rn episodes observed at Crozet Island in the Indian Ocean, demonstrating that they can resolve the synoptic-scale transport of continental plumes with no significant numerical diffusion. Large differences between models are found in the rates of meridional transport in the upper troposphere (interhemispheric exchange, exchange between tropics and high latitudes). The four two-dimensional models which participated in the intercomparison tend to underestimate the rate of vertical transport from the lower to the upper troposphere but show concentrations of ^{222}Rn in the lower troposphere that are comparable to the zonal mean values in the three-dimensional models.

[1] Division of Engineering and Applied Sciences and Department of Earth and Planetary Sciences, Harvard University, Cambridge, Massachusetts.
[2] Department of Geoscience, University of California at Irvine, Irvine.
[3] National Center for Atmospheric Research, Boulder, Colorado.
[4] AER Incorporated, Cambridge, Massachusetts.
[5] Laboratoire de Modèlisation du Climat et de l'Environnement, CEA, Gif sur Yvette, France.
[6] York University, North York, Ontario, Canada.
[7] Lawrence Livermore National Laboratory, Livermore, California.
[8] NASA Langley Research Center, Hampton, Virginia.
[9] Department of Applied Mathematics, University of Washington, Seattle.
[10] Now at Aculight Corporation, Bellevue, Washington.
[11] Second Laboratory of Climate Research Devision, Meteorological Research Institute, Nagamine, Tsukuba, Ibaraki, Japan.
[12] Department of Chemistry, University of Cambridge, Cambridge , England.
[13] Max-Planck-Institut für Meteorologie, Hamburg, Germany.
[14] Laboratoire de Glaciologie et Géophysique de l'Environnement, Centre National de la Recherche Scientifique, Saint Martin d'Hères, France.
[15] School of Earth and Atmospheric Sciences, Georgia Institute of Technology, Atlanta.

Paper number 96JD02955.
0148-0227/97/96JD-02955$09.00

[16] Institut für Physik der Atmosphäre, Deutsche Luft und Raumfahrt Mitteilung, Oberpfaffenhofen, Germany.
[17] Atmospheric Sciences Research Center, State University of New York at Albany.
[18] Centre des Faibles Radioactivités, Laboratoire mixte CNRS/Commissariat à l'Energie Atomique, Gif-sur-Yvette, France.
[19] School of Environmental Sciences, University of East Anglia, Norwich, England.
[20] Royal Netherlands Meteorological Institute (KNMI), De Bilt.
[21] MOGUNTIA Global Modelling, Raunheim, Germany.

1. Introduction

Convective and synoptic processes play a major role in the global transport of heat, momentum, and trace gases in the atmosphere. Capturing these processes in global models is a challenge because of the coarse resolution of the models (typically 100-1000 km in the horizontal). Convection is subgrid on these scales and must be parameterized. Synoptic motions are near the grid scale. We report here on an intercomparison sponsored by the World Climate Research Program (WCRP) in 1993 to evaluate the capability of global models to capture the contributions of convective and synoptic processes to transport on a global scale. Twenty models from seven countries participated (Table 1 and Appendix). Sixteen of the models were three-dimensional and four were zonally averaged two-dimensional. Most had a recorded history of use prior to the intercomparison and are

Table 1. Participants in the Intercomparison

Model	Contributor
Established Three-Dimensional Synoptic Models	
A. CCM2	Rasch
B. ECHAM3	Feichter, Köhler
C. GFDL/ZODIAC	Kasibhatla
D. GISS/H/I	Jacob
E. KNMI/TM2	Verver, Van Velthoven
F. LLNL/GRANTOUR	Dignon, Penner
G. LLNL/E	Bergmann
H. LMD	Genthon
I. TM2Z	Balkanski, Ramonet
Established Nonsynoptic Three-Dimensional Model	
J. MOGUNTIA	Zimmermann
Three-Dimensional Synoptic Models Under Development	
k. CCC-GCM	Beagley, de Grandpré
m. LaRC	Grose, Blackshear
n. LLNL/IMPACT	Rotman
o. MRI	Chiba
p. TOMCAT	Chipperfield
q. UGAMP	Stockwell
Two-Dimensional Models	
R. AER	Shia
S. UCAMB	Law, Wild
T. HARWELL	Reeves
U. UW	Brown, Yang

A description of each model is given in the Appendix. Models are called "synoptic" if they use meteorological fields with temporal resolution finer than 1 day. MOGUNTIA uses monthly mean winds.

referred to as "established." Others were still under development at the time of the intercomparison and are identified as such in Table 1.

The intercomparison consisted of simulations of three short-lived tracers. Primary focus was on ^{222}Rn, a natural radioisotope emitted ubiquitously from soils by decay of ^{226}Ra [*Nazaroff*, 1992] and removed from the atmosphere by radioactive decay with an e-folding lifetime of 5.5 days. Because of its simple source and sink, ^{222}Rn has long been recognized as a useful tracer of convective and synoptic-scale motions in global models [*Brost and Chatfield*, 1989; *Feichter and Crutzen*, 1990; *Jacob and Prather*, 1990; *Allen et al.*, 1996; *Mahowald et al.*, 1996; *Ramonet et al.*, 1996; *Rind and Lerner*, 1996]. A comparative analysis of two general circulation models (GCMs) using ^{222}Rn as a diagnostic tracer was reported by *Genthon and Armengaud* [1995a].

Also included in the intercomparison were simulations of two fictitious short-lived tracers with sources at 400-200 hPa. These simulations were aimed at examining downward transport and horizontal motions in the upper troposphere, complementing the ^{222}Rn simulation. Results could not be compared to observations but still allowed an assessment of differences between models.

All participants in the intercomparison were requested to submit their results to an organizing committee (M. Prather, B. Boville, and D. Jacob) prior to an intercomparison workshop which was held on November 30 to December 3, 1993, and was attended by representatives of almost all models. Participants were not allowed to revise their submitted results after the workshop except for correcting errors in input conditions and output diagnostics.

2. Simulations

Specifications for each simulation are given in Table 2. The ^{222}Rn simulation (case A) assumed a uniform emission of 1.0 atoms cm^{-2} s^{-1} from land, excluding polar regions. This source is thought to be accurate to within 25% globally [*Turekian et al.*, 1977; *Balkanski et al.*, 1993] and to within a factor of 2 regionally [*Wilkening et al.*, 1975; *Schery et al.*, 1989; *Graustein and Turekian*, 1990; *Nazaroff*, 1992]. The dominant causes of variability of ^{222}Rn emission are the ^{226}Ra abundance in soil, the location of ^{226}Ra within the soil grains, soil moisture, and soil freezing [*Jacob and Prather*, 1990; *Nazaroff*, 1992]. Data are lacking to describe these effects globally, hence there is little justification for using a more complicated source function than that given in Table 2. Ignoring the effect of soil freezing overestimates ^{222}Rn emission at high latitudes in winter [*Dörr and Munnich*, 1990; *Jacob and Prather*, 1990; *Genthon and Armengaud*, 1995a]. The oceanic source of 0.005 atoms cm^{-2} s^{-1} in Table 2 is an upper limit [*Wilkening and Clements*, 1975; *Lambert et al.*, 1982] but is unimportant except for defining background concentrations of ^{222}Rn in the marine boundary layer. Loss of ^{222}Rn is solely by radioactive decay with a first-order rate constant $k = 2.1 \times 10^{-6}$ s^{-1}.

Cases B and C used fictitious tracers with the same first-order loss rate constant as ^{222}Rn but with sources in the upper troposphere (400-200 hPa) at northern midlatitudes and in the tropics, respectively. These tracers were intended to be illustrative of emissions from aircraft (case B) and tropical lightning (case C).

The simulations were conducted for two 4-month periods, May-August and November-February, starting from zero tracer concentrations as initial conditions. The first month was used for initialization, and model output was sampled for the last 3 months. Since different models used different meteorological years, we focus our comparison on seasonal statistics of tracer concentrations; however, interannual variability of weather remains a confounding factor. We will use interannual ranges of observed seasonal statistics, when available, to define the expected range of interannual variability in the models.

3. Case A (^{222}Rn): Comparisons with observations

Reviews of the database of ^{222}Rn measurements in the atmosphere have been presented by *Lambert et al.* [1982], *Liu et al.* [1984], and *Gesell* [1983]. We use observations for Cincinnati (United States), Crozet Island (Indian Ocean), and Hawaii (200 hPa) as offering the best seasonal statistics for model evaluation in continental interior, marine air, and upper troposphere environments (Table 3). Mean vertical profiles of observed ^{222}Rn concentrations over northern midlatitude continents [*Liu et al.*, 1984] are also used for model evaluation. The ^{222}Rn concentrations throughout this paper are expressed in units of molar mixing ratios (mol/mol). Conversion factors to common radioactivity units are 1×10^{-21} mol/mol = 1.52 pCi/m^{3}STP = 5.6×10^{-2} Bq/m^{3}STP where "pCi" is picocuries, "Bq" is becquerels, and "m^{3}STP" is a standard cubic meter of air at 273.15 K and 1 atm.

Cincinnati, United States

Cincinnati is in the continental interior of the United States, where ^{222}Rn concentrations are controlled primarily by vertical mixing of the continental boundary layer. *Gold et al.* [1964] reported 4 years of continuous ^{222}Rn measurements made 1.5-m above ground at 0800 and 1500 local time (LT). We limit our attention to the data at 1500 LT, when surface measurements are most likely to be representative of a mixed layer resolved by the models, and to the summer season, when ^{222}Rn emission is unaf-

Table 2. Tracer Source Distributions

	Altitude	Latitude	Longitude	Source
Case A	Earth surface	70°-90°	all	0
^{222}Rn	ibidem	60°-70°	all	0.005 atoms cm^{-2} s^{-1}
	ibidem	60°S-60°N	oceans	0.005 atoms cm^{-2} s^{-1}
	ibidem	60°S-60°N	land	≈1.0 atoms cm^{-2} s^{-1} [a]
Case B	400-200 hPa	34°N	120°E-120°W	18 mol yr^{-1} [b]
Aircraft tracer	ibidem	40°N	120-75°W	18 mol yr^{-1}
	ibidem	42°N	75°W-10°E	18 mol yr^{-1}
	ibidem	42-60°N	10°E	18 mol yr^{-1}
Case C	400-200 hPa	10°S-10°N	75-45°W	24 mol yr^{-1} [c]
Tropical lightning	ibidem	10°S-10°N	10-40°E	24 mol yr^{-1}
tracer	ibidem	10°S-10°N	100-130°E	24 mol yr^{-1}

[a] Participants were requested to adjust their ^{222}Rn emission flux from land at 60°S-60°N to yield a global ^{222}Rn source of 72 mol yr^{-1}; the reason for this adjustment is that global land area may differ between models. Consider a model with a total surface area of 37.8 x 10^6 km^2 at 60°-70° (^{222}Rn source 0.10 mol yr^{-1}), a total ocean area of 315x10^6 km^2 at 60°S-60°N (^{222}Rn source 0.83 mol yr^{-1}), and a total land area of 127x10^6 km^2 at 60°S-60°N. The total source of land at 60°S-60°N in this model must be 71.07 mol yr^{-1}, so that the ^{222}Rn emission flux from land should be specified as 1.07 atoms cm^{-2} s^{-1}.

[b] Emitted uniformly and at a constant rate horizontally along the specified line segment and vertically from 400 to 200 hPa along the pressure coordinate. The four line segments in case B have unequal lengths, but the total source of tracer for each segment is the same (hence the emission flux is higher for the shorter segments). The global source of tracer is 72 mol yr^{-1}.

[c] Emitted uniformly and at a constant rate over the specified horizontal domain and vertically from 400 to 200 hPa along the pressure coordinate. The three source regions in case C all have the same volume. The global source of tracer is 72 mol yr^{-1}.

Table 3. Radon 222 Concentration Measurements

Site	Measurement period	Diagnostic variable	^{222}Rn Concentration, 10^{-21} mol/mol
Cincinnati	June-Aug. 1959-1962	June-Aug. mean at	75 (1959), 90 (1960),
40°N, 84°W		1500LT	92 (1961), 103 (1962)[a]
Crozet Island	June-Aug. 1968-1994[b]	seasonal minimum	<0.1
46°S, 51°E		first quartile	0.5
		median	0.8
		third quartile	1.3
		seasonal maximum[c]	23 (13-36)
Hawaii, 200 hPa	July-Aug. 1983-1984[d]	minimum	<0.7
20°N, 155°W		first quartile	<0.7
		median	2.5
		third quartile	5.3
		maximum	26

Observations from *Gold et al.* [1964] at Cincinnati, *Lambert et al.* [1995] at Crozet, and *Kritz et al.* [1990] at Hawaii. See text for conversion factors from molar mixing ratios (mol/mol) to common radioactivity units.

[a] Mean June-August concentration at 1500 local time (LT) for each of the 4 years of observations.

[b] Continuous record of hourly data. Data for 1981-1985 are missing.

[c] Median value and interannual range of the seasonal maximum concentration for the individual years of the 22-year record.

[d] Seventeen samples collected from aircraft on flights between 18° and 25°N in the vicinity of Hawaii. Each sample was of 30-min duration, corresponding to a 250-km averaging distance along the aircraft flight track. The individual measurements are reported by *Balkanski et al.* [1992].

fected by soil freezing. The mean June-August concentrations at 1500 LT measured by *Gold et al.* [1964] range from 75 to 103 x 10^{-21} mol/mol for the 4 years of measurements (Table 3).

We compare in Figure 1 the summer afternoon mean concentrations computed by the models at Cincinnati (white bands) to the interannual range of the observed means (dashed lines). Model results were archived at 1400 LT and 300 m altitude; this altitude was chosen so that the intercomparison would not be affected by differences between models in details of vertical gridding near the surface. In the models that resolve the atmosphere below 300 m altitude, summer afternoon concentrations at 300 m are about 20% lower than at 1 m.

The results in Figure 1 show that most three-dimensional models agree with the observations to within the uncertainty on the ^{222}Rn emission flux. The two-dimensional models (R-U) are low because of zonal averaging of the ^{222}Rn source over land and ocean. Concentrations in CCM2 (A), MOGUNTIA (J), and LLNL/IMPACT (n) are only slightly higher than in the two-dimensional models and lower than observed, implying excessive boundary layer heights. Subsequent versions of CCM2 are improved in that regard (P. J. Rasch, personal communication, 1996). Concentrations in ECHAM3 [B] are higher than observed, implying insufficient boundary layer mixing.

Gold et al. [1964] give no information on the day-to-day variability of ^{222}Rn concentrations at Cincinnati. All three-dimensional synoptic models in Figure 1 show remarkably similar variability except for ECHAM3 (B), MRI [o], TOMCAT [p], and UGAMP [q], which have frequent occurrences of anomalously high concentrations. MOGUNTIA, which uses monthly mean winds, does not have day-to-day variability.

Crozet Island, Indian Ocean

Crozet is located in the subantarctic Indian Ocean 2800 km from the African coast. Twenty-two years of hourly ^{222}Rn measurements at the site are available as an electronic archive [*Lambert et al.*, 1995]. The data indicate a low background of 0.1-1 x 10^{-21} mol/mol interrupted about once a month by high-^{222}Rn episodes lasting typically 1-2 days [*Lambert et al.*, 1970; *Polian et al.*, 1986]. The episodes are caused by fast boundary layer transport of air from Africa channeled between the semipermanent Mascarene High over the subtropical Indian Ocean and transient cyclones at southern midlatitudes [*Balkanski and Jacob*, 1990; *Heimann et al.*, 1990; *Miller et al.*, 1993]. The strongest episodes occur in austral winter when the Mascarene High is close to the African coast. The June-August seasonal maximum ^{222}Rn concentration measured at Crozet ranges from 13 to 36x10^{-21} mol/mol for the 22 years of observations (Table 3).

We see from Figure 1 that all established three-dimensional synoptic models reproduce the observed pattern of low ^{222}Rn background concentrations at Crozet interrupted occasionally by high-^{222}Rn episodes. Inspection of the time series in the individual models indicates between 3 and 8 high-^{222}Rn episodes at Crozet during June-August, each lasting typically 1-2 days, and

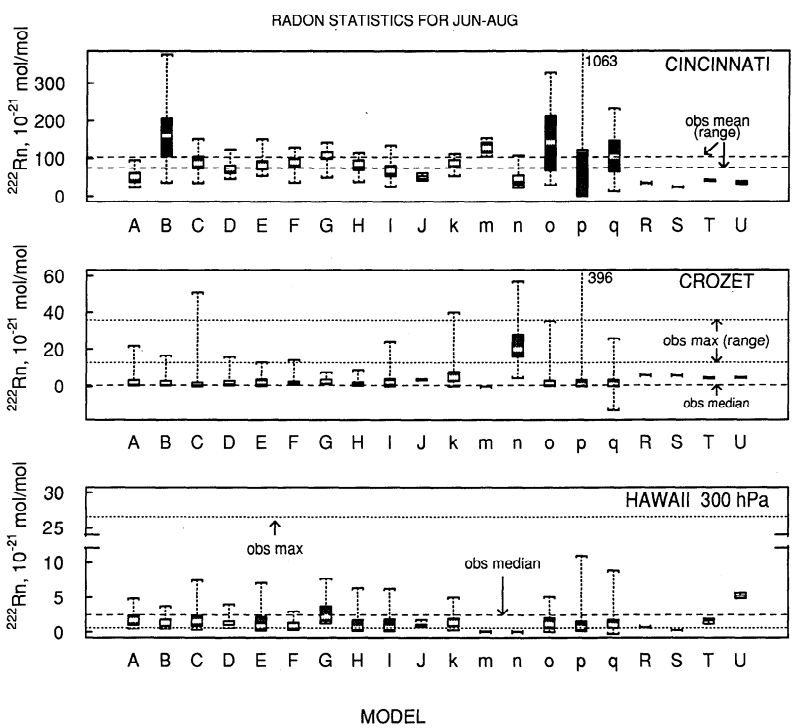

Figure 1. Frequency distributions of simulated ^{222}Rn concentrations at Cincinnati (300 m altitude, 1400 LT), Crozet Island (ibidem), and Hawaii (300 hPa, all times of day) for the summer season (June-August). See text for conversion of molar mixing ratios (mol/mol) to common radioactivity units. Models are identified by letter code (see Table 1). Values for the two-dimensional models (R-U) are zonal mean concentrations. Box plots for each model show seasonal extrema (whiskers) and quartiles (shaded box); the white band indicates either the seasonal mean concentration (Cincinnati) or the median (Crozet, Hawaii). Dashed lines in the Cincinnati panel show the interannual range of the observed June-August mean concentration at 1500 LT (4 years of data). Dotted lines in the Crozet panel show the interannual range of the observed seasonal maximum concentration (22 years of data), and the dashed line shows the observed median concentration. Dotted and dashed lines in the Hawaii panel show, respectively, the extrema and median concentrations in 17 aircraft samples collected at 200 hPa; note the break in the ordinate scale. The minimum indicated by the dotted line (0.7 x 10^{-21} mol/mol) is the detection limit of the instrument. See text and Table 3 for further information concerning the observations.

none lasting longer than 3 days. The seasonal maxima of ^{222}Rn in the models are within the interannual range of observed values except in GFDL/ZODIAC (C) where one episode is anomalously high, and in LLNL/E (G) and LMD (H) where the episodes are somewhat too weak. The generally good simulation of the structure and magnitude of high-^{222}Rn episodes suggests that the models resolve the synoptic-scale transport of ^{222}Rn from Africa to Crozet and that they can transport the African plume over the ocean for several days without appreciable numerical diffusion. The median concentrations in the models ($1\text{-}2\times10^{-21}$ mol/mol) are higher than observed, probably due to an excessive oceanic source in the simulations rather than to numerical diffusion.

Among the three-dimensional models under development, only MRI (o) yields statistics comparable to the established three-dimensional models. CCC-GCM (k) and especially LLNL/IMPACT (n) have too high medians; LaRC (m) does not simulate high-^{222}Rn episodes; TOMCAT (p) has an anomalously high maximum; and UGAMP (q) produces negative concentrations. The two-dimensional models yield higher ^{222}Rn concentrations at Crozet than the three-dimensional models because of inclusion of the South American landmass in the zonal means at 46°S (latitude of Crozet). Inspection of zonal mean concentrations at 46°S indicates agreement to within a factor of 2 between the two-dimensional models and the established three-dimensional models. MOGUNTIA (J), which uses a 10° x 10° horizontal resolution, shows median concentrations at Crozet that are comparable to the two-dimensional models and higher than observed, suggesting that the model resolution is too coarse to capture the gradient between the African continent and the island. *Genthon and Armengaud* [1995a] reported previously a similar problem when using the GISS GCM with 8° x 10° resolution to simulate high-^{222}Rn episodes at Kerguelen Island, near Crozet; the simulation is better when the 4°x5° resolution version of the same GCM is used [*Balkanski and Jacob*, 1990].

Upper Troposphere Over Hawaii

Kritz et al. [1990] reported 61 aircraft measurements of ^{222}Rn concentrations at 200 hPa over the North Pacific between California and Hawaii in July-August 1983-1984. Seventeen of these measurements were made in the vicinity of Hawaii at 18°-25°N. Each measurement was of 30-minute duration, corresponding to an averaging distance of about 250 km. The median concentration for the 17 Hawaii measurements was 2.5×10^{-21} mol/mol; 3 of the 17 measurements were higher than 10×10^{-21} mol/mol, and the highest measurement was 26×10^{-21} mol/mol. *Kritz et al.* [1990] showed that the occurrences of extremely high concentrations were due to deep convection over eastern Asia followed by rapid transport of this continental air over the Pacific in the subtropical jet.

The frequency distributions of ^{222}Rn concentrations simulated by the different models at 300 hPa over Hawaii in summer are shown in the bottom panel of Figure 1. The observed median and extrema of *Kritz et al.* [1990] at 200 hPa are superimposed as dashed and dotted lines, respectively. Only the 300 hPa time series were archived in the models; the difference between summer mean concentrations at 300 hPa and 200 hPa over Hawaii in individual models is less than 30%, so it seems appropriate to compare the model statistics at 300 hPa to the measured values at 200 hPa. We see from Figure 1 that all three-dimensional models underestimate the observed median concentrations by typically a factor of 2. The maxima are underestimated by a greater factor; that is, the models do not capture the large relative variability in the observations. Concentrations simulated by LaRC [m] and LLNL/IMPACT [n] never exceed 0.1 x 10^{-21} mol/mol, which may be explained by the lack of a subgrid convective parameterization to transport ^{222}Rn to high altitudes in these models. All two-dimensional models except UW [U] show concentrations lower than the observed median.

One possible explanation for the failure of the three-dimensional models to reproduce the high concentrations observed over Hawaii would be the presence of an anomalously high ^{222}Rn source in eastern Asia. This explanation has been proposed by P. Kasibhatla and N. Mahowald (personal communication, 1996) to account for measurements of elevated ^{222}Rn concentrations at Mauna Loa Observatory, Hawaii. There are, to our knowledge, no measurements of ^{222}Rn concentrations or emission fluxes over eastern Asia, but ^{210}Pb deposition fluxes measured at sites in China and Japan indicate values more than double those found anywhere in the United States or Europe [*Fukuda and Tsunogai*, 1975; *Preiss et al.*, 1996]. An underestimate of ^{222}Rn emission in eastern Asia may still not explain why the models underestimate the relative variability of ^{222}Rn concentrations over Hawaii; this latter problem may be due in part to the coarse vertical gridding used by the models in the upper troposphere.

Vertical Profiles Over Continents

Seasonal mean vertical profiles of ^{222}Rn concentrations over northern midlatitude continents have been compiled by *Liu et al.* [1984] by averaging together measurements made at different locations in North America and Europe. The data are scant, consisting of 23 profiles at 6 locations in summer and 7 profiles at 3 locations in winter. We compare these data in Figure 2 to model results at 300 m above ground (mixed layer), 600 hPa, and 300 hPa for the three continental midlatitude sites where model time series were archived: Cincinnati (40°N, 84°W) and Socorro (34°N, 107°W), United States; and Kirov (58°N, 49°E), Russia. Mean values and standard errors ($\sigma/\sqrt{n}$) from the *Liu et al.* [1984] compilation are shown for the corresponding altitudes.

We find that most of the established three-dimensional models reproduce the observed vertical profiles to within a factor of 2 at all altitudes. Exceptions are LLNL/E (G) in summer, where concentrations at 300 hPa are too low, and ECHAM3 (B), where mixed layer concentrations are a factor of 2 higher than in other established three-dimensional models for both summer and winter. Uncertainty in the effect of soil freezing (not accounted for in the models) introduces some ambiguity in the wintertime comparison.

Considerable underestimate of concentrations in the middle and upper troposphere is found in three-dimensional models under development that do not include a subgrid parameterization of convective transport: LaRC (m), LLNL/IMPACT (n), and TOMCAT (p). This result emphasizes the importance of convective parameterizations in three-dimensional models. The two-dimensional models generally underestimate the observations, as would be expected simply due to zonal averaging of concentrations; however, UW (U) overestimates concentrations in the middle and upper troposphere in winter, implying excessive vertical mixing.

Deep convective transport over continents is an episodic process, and concentrations of continental tracers in the upper troposphere are known to be highly variable. There are few ^{222}Rn observations available in the upper troposphere over continents to evaluate model variability. The largest single source of upper troposphere data in the compilations of *Liu et al.* [1984] is from four aircraft flights over eastern Ukraine in July [*Nazarov et al.*, 1970]. We compare in Figure 3 the range of values reported by *Nazarov et al.* [1970] at 300 hPa to the summertime frequency distributions simulated by the established three-dimensional synoptic models at the same altitude over Kirov. The seasonal ranges in the models encompass the range defined by the observations but not by much. Considering that the observational range is defined by just four measurements, while the model ranges are from continuous sampling over a 3-month time period, it appears that the three-dimensional models probably underestimate the variability of ^{222}Rn in the continental upper tropo-

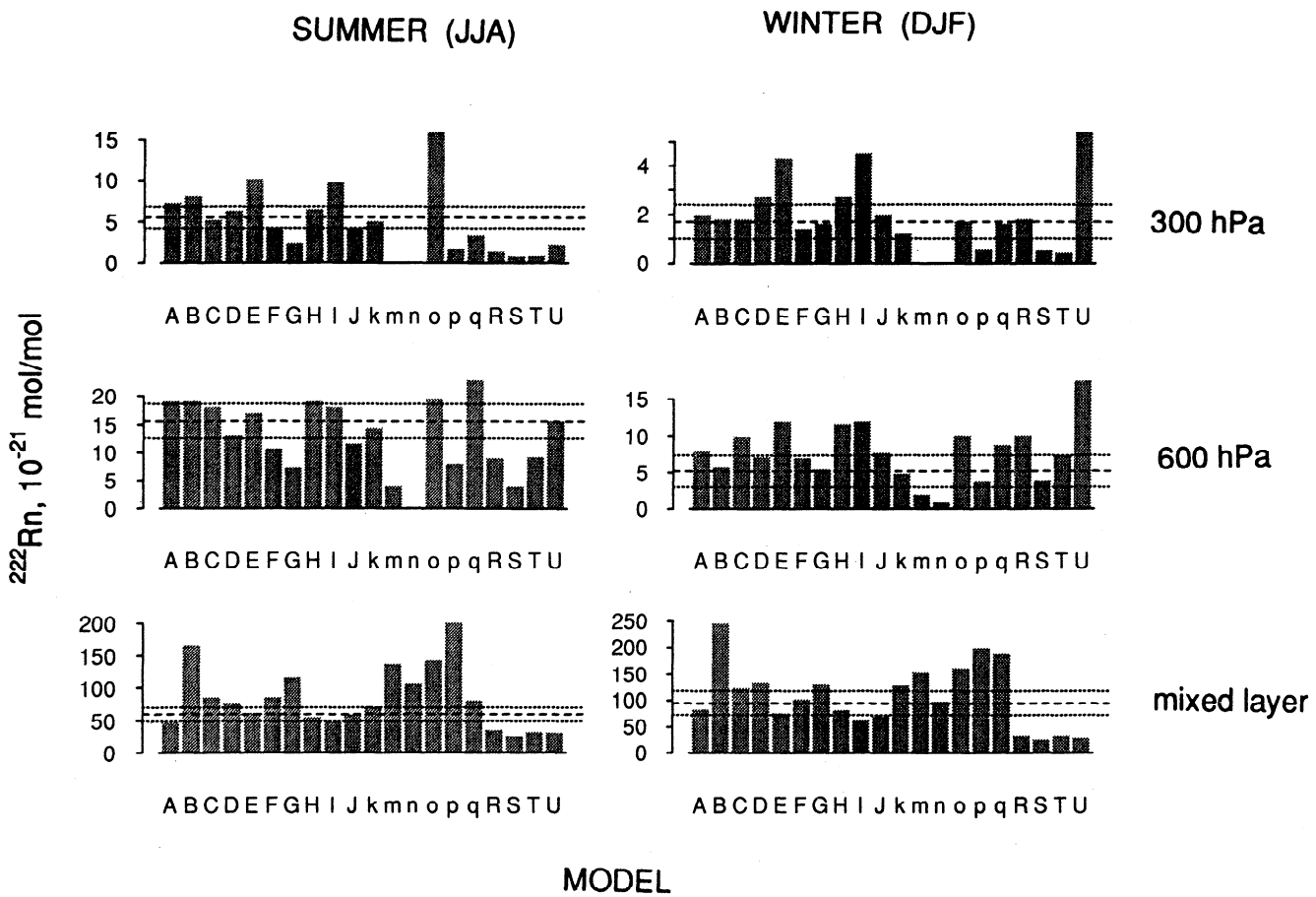

Figure 2. Mean ^{222}Rn concentrations over northern midlatitude continents at 300 m altitude (mixed layer), 600 hPa, and 300 hPa in June-August and December-February. The dashed lines are averages of aircraft observations from various locations in North America and Europe, and the dotted lines are the corresponding standard errors $\sigma/\sqrt{n}$ (standard deviations on the means) [*Liu et al.*, 1984]. Model results are averages over the three midlatitude continental sites for which model time series were archived: Cincinnati (40°N, 84°W), Socorro (34°N, 107°W), and Kirov (58°N, 49°E). The models are identified by the letter code of Table 1.

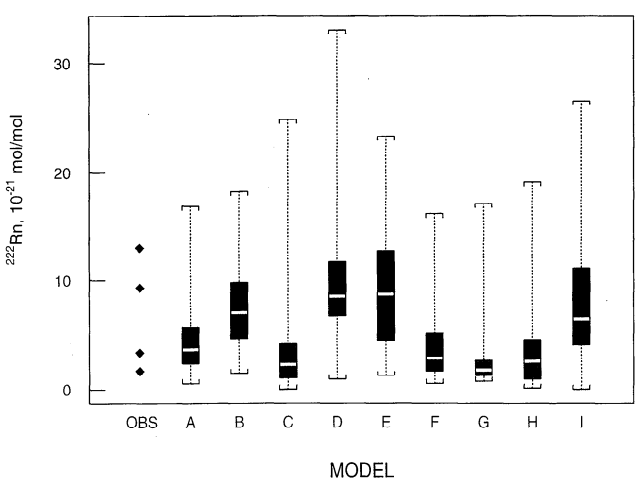

Figure 3. Frequency distribution of ^{222}Rn concentrations measured at 300 hPa during four aircraft flights over eastern Ukraine in July ("OBS" column) and simulated by the established three-dimensional synoptic models at 300 hPa over Kirov in June-August (box plots). The diamonds in the "OBS" column are the individual measurements reported by *Nazarov et al.* [1970]. The box plots show seasonal extrema (whiskers), quartiles (shaded box), and medians (white band) of the 3-month time series in the individual models. The models are identified by the letter code of Table 1.

sphere. This result would be consistent with the previously discussed model underestimate of ^{222}Rn variability in the marine upper troposphere over Hawaii.

4. Cases A-C: Global Distributions

Global distributions of seasonally averaged concentrations allow a more general intercomparison of model results. We limit further analysis to the established models and to CCC-GCM; as pointed out above, some of the models under development exhibited major anomalies when compared to observations. LMD did not report zonal mean concentrations and their data are therefore missing from the corresponding figures below.

Figure 4 compares the ^{222}Rn concentration maps at 300 hPa in June-August for the different three-dimensional models. All models show remarkably similar distributions reflecting convective pumping of ^{222}Rn over continents followed by long-range transport over the oceans. Exceptions are MOGUNTIA, CCC-GCM, and the LLNL models (especially the Eulerian version, LLNL/E), where ^{222}Rn concentrations are generally a factor of 2 lower than in the other models. ECHAM3 shows particularly high concentrations in polar regions, reflecting strong meridional transport from middle to high latitudes in the upper troposphere.

Zonal mean cross sections of ^{222}Rn concentrations as a function of altitude and latitude in June-August are compared in Figure 5. Results for the three-dimensional models are highly similar as seen, for example, in the patterns of deep convection in the tropics, midlevel convection at northern midlatitudes, and meri-

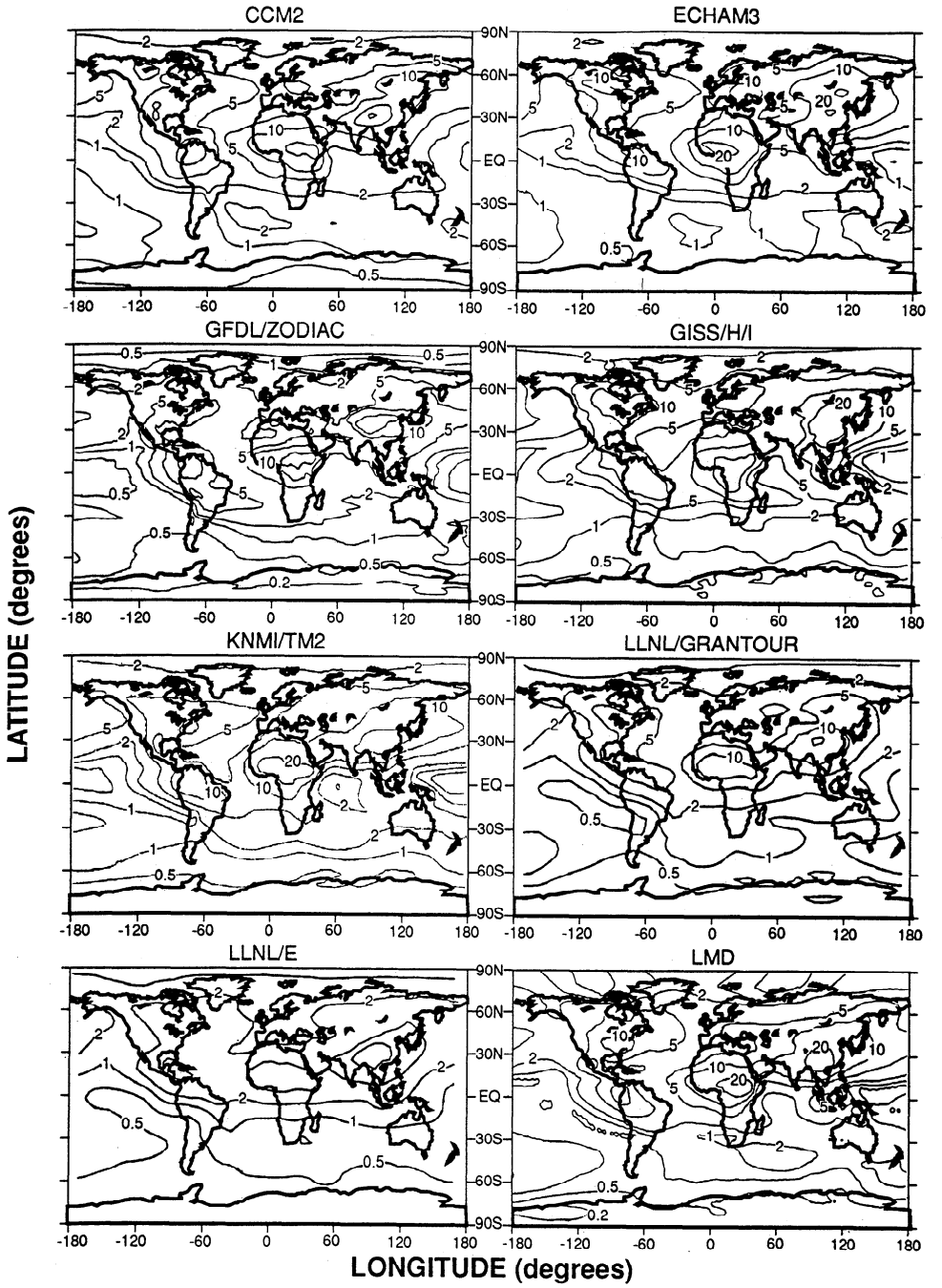

Figure 4. Mean ^{222}Rn concentrations simulated by the different models at 300 hPa in June-August. Units are 1 x 10^{-21} mol/mol; see text for conversion factors.

dional gradients in the lower and middle troposphere. GISS/H/I features a secondary maximum of concentrations in the equatorial upper troposphere due to frequent deep convection, but none of the other models show such a maximum. All two-dimensional models except UW underestimate concentrations in the upper troposphere, a problem likely caused by inadequate treatment of convection. Results for UW are close to those of the three-dimensional models.

Zonal mean cross sections of concentrations for the aircraft tracer (case B) in June-August are presented in Figure 6. All three-dimensional models show similar vertical gradients at northern midlatitudes, implying similar rates of downward transport, except KNMI/TM2 where this transport is unusually rapid. Large differences between three-dimensional models are found in the rates of meridional transport in the upper troposphere. GISS/H/I and ECHAM3 have the slowest interhemispheric transport at high altitudes, resulting in tracer concentrations in the southern tropics that are 1 order of magnitude lower than in the LLNL models and CCM2, where interhemispheric transport is particularly rapid. Transport from northern midlatitudes to the Arctic in the upper troposphere also varies considerably between three-dimensional models; concentrations in the Arctic differ by more than 1 order of magnitude between MOGUNTIA (where transport is fastest) and GFDL/ZODIAC (slowest). A more recent version of MOGUNTIA yields tracer concentrations over the Arctic that are more consistent with the other three-dimensional models (P. Zimmermann, personal communication, 1996). The zonal mean cross sections of concentrations in the

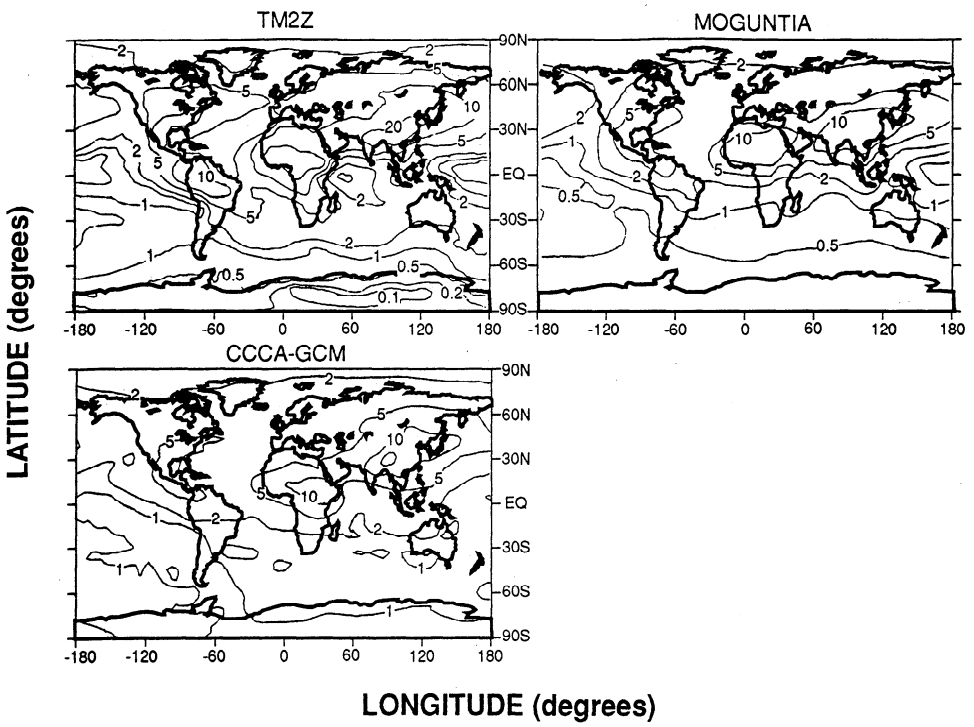

Figure 4. (continued)

two-dimensional models are generally within the range of results from the three-dimensional models, although the latitude of maximum downward transport is displaced in UW.

Figure 7 shows the zonal mean cross sections of concentrations in December-February for the tropical lightning tracer (case C). All synoptic three-dimensional models show similar vertical gradients in the tropics, implying again close similarity in the computed rates of downward transport. MOGUNTIA features tracer concentrations in the lower tropical troposphere that are 5 times higher than the synoptic three-dimensional models. A more recent version of MOGUNTIA shows improvement (P. Zimmermann, personal communication, 1996). As in case B, meridional transport rates from the tropics to high latitudes in the upper troposphere vary considerably between three-dimensional models. Downward transport in the tropics in the two-dimensional models is too fast in UW and too slow in AER and UCAMB. Meridional transport rates in the two-dimensional models are consistent with the range of values in the three-dimensional models.

5. Conclusions

Simulations of ^{222}Rn and other short-lived tracers have provided a number of insights into the ability of global atmospheric models to capture the contributions of convective and synoptic processes to global-scale transport. Results show that most established three-dimensional synoptic models simulate boundary layer mixing and deep convection in the troposphere to within the constraints offered by observed seasonal averages of ^{222}Rn concentrations at different altitudes. Subgrid parameterization of convection is essential; the three-dimensional models under development that did not include such a parameterization underestimated considerably the observed ^{222}Rn concentrations in the upper troposphere. Comparison of zonal mean ^{222}Rn concentrations simulated by the two-dimensional versus three-dimensional models indicates that the 2-D models offer a good simulation of large-scale meridional transport in the troposphere but fail to reproduce the vertical gradients obtained by the three-dimensional models, presumably because they do not account adequately for deep convection.

Almost all established three-dimensional synoptic models reproduce the observed seasonal statistics of high-^{222}Rn episodes at Crozet Island, 2800 km away from the African coast. The amplitudes, durations (1-2 days), and frequencies of the episodes are well simulated. We conclude that the models can resolve the synoptic weather systems responsible for the high-^{222}Rn episodes and can carry continental plumes for several days over the ocean with little numerical diffusion.

The largest discrepancies between established three-dimensional models and observations are found in the simulation of ^{222}Rn in the upper troposphere. None of the models can reproduce the high ^{222}Rn concentrations observed at 200 hPa over Hawaii, and none shows sufficient day-to-day variability of ^{222}Rn concentrations in the upper troposphere. Large differences are found between established three-dimensional models in the rates of global-scale meridional transport in the upper troposphere, including in particular interhemispheric transport.

Appendix: Description of the Participating Models

A. NCAR CCM2

This three-dimensional tracer model uses instantaneous meteorological fields from the standard version of the CCM2 [*Hack*, 1993; *Hack et al.*, 1993, 1994]. Horizontal resolution is 2.8° x 2.8°. Vertical resolution is 18 layers up to 5 hPa, with 11 in the troposphere. Time step is 15 minutes. Convective mass fluxes are calculated as described by *Hack* [1994]. The scheme adjusts the moist static energy over three adjacent layers, allowing for entrainment in the bottom layer, condensation and rain out in the middle layer, and detrainment in the top layer. The method is applied sequentially, beginning at the surface, until all of the tropospheric levels have been adjusted. Resolved scale transport is performed using a shape preserving semi-Lagrangian transport algorithm [*Rasch and Williamson*,, 1990]. A nonlocal boundary layer parameterization [*Holtslag and Boville*, 1993] diagnoses a

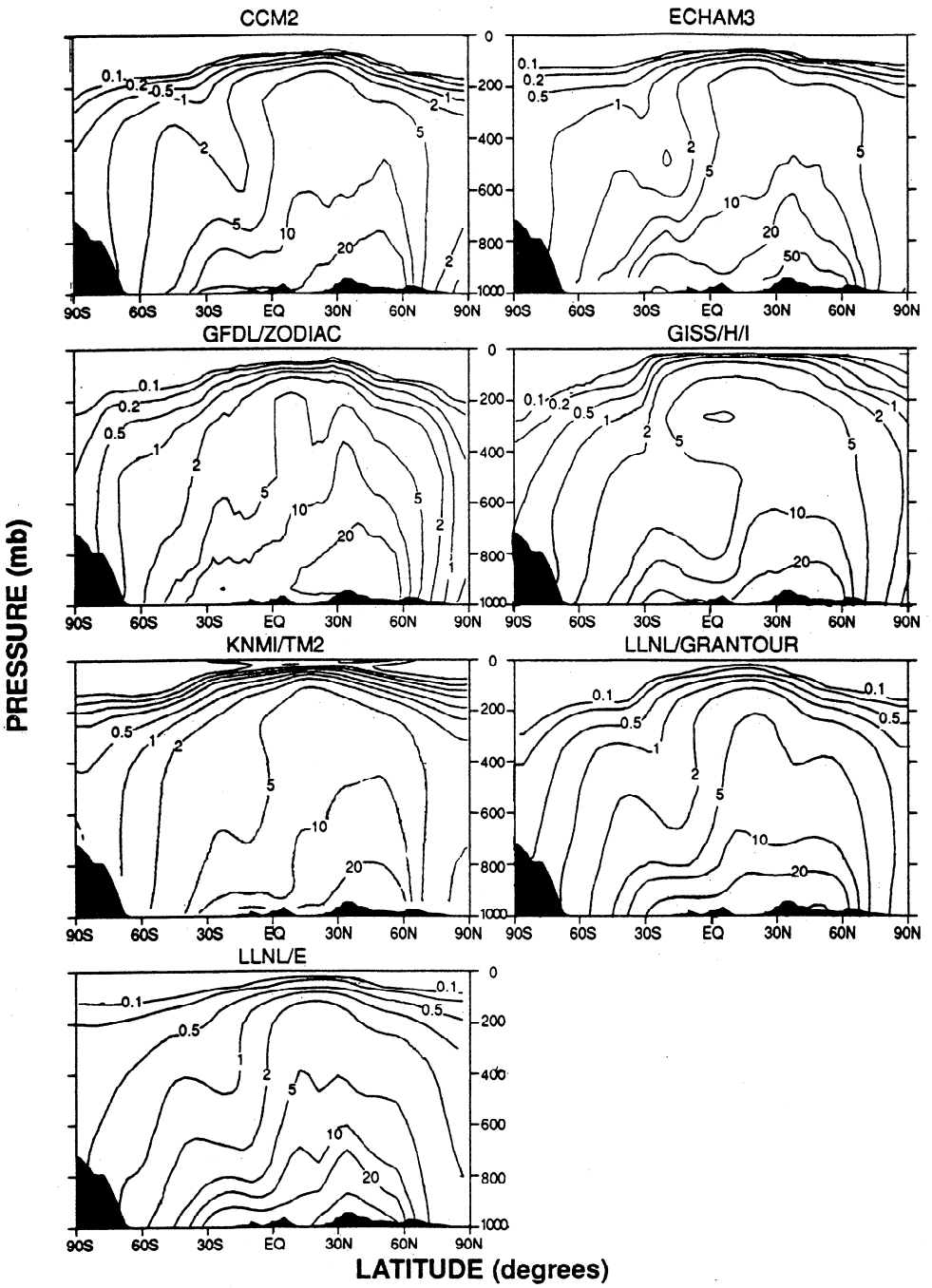

Figure 5. Zonal mean ^{222}Rn concentrations (units of $1x10^{-21}$ mol/mol) simulated by the different models in June-August.

boundary layer depth and determines diffusivity profiles and nonlocal turbulent transports of heat and constituents within the boundary layer. These algorithms have been used in a variety of chemical transport studies [i.e., *Rasch et al.*, 1994, 1995; *Hartley et al.*, 1994].

B. ECHAM3

This GCM uses spectral transport with triangular truncation (T21) [*Roeckner et al.*, 1992]. Nonlinear and physical terms are calculated on a Gaussian grid (5.6°x5.6°). Vertical resolution is 19 levels up to 10 hPa. Model time step is 40 min. Advection of water vapor, cloud water, and chemicals is done with a semi-Lagrangian method [*Rasch and Williamson*, 1990]. Surface fluxes of momentum, heat, moisture, and trace gases are calculated from Monin-Obukhov theory. Turbulent transfer is calculated using a higher-order closure scheme. The convection mass flux scheme is from *Tiedtke* [1989]. The model has been used in many studies of climate sensitivity [*Cess et al.*, 1990; *Cubasch et al.*, 1992; *Roeckner et al.*, 1995], tracer transport [*Brost et al.*, 1991; *Feichter et al.*, 1991a, b] and tropospheric chemistry [*Roelofs and Lelieveld*, 1995; *Feichter et al.*, 1996].

C. GFDL/ZODIAC

This three-dimensional tracer model uses 6-hour time-average meteorological fields from a Geophysical Fluid Dynamics Laboratory GCM [*Manabe et al.*, 1974]. Horizontal resolu-

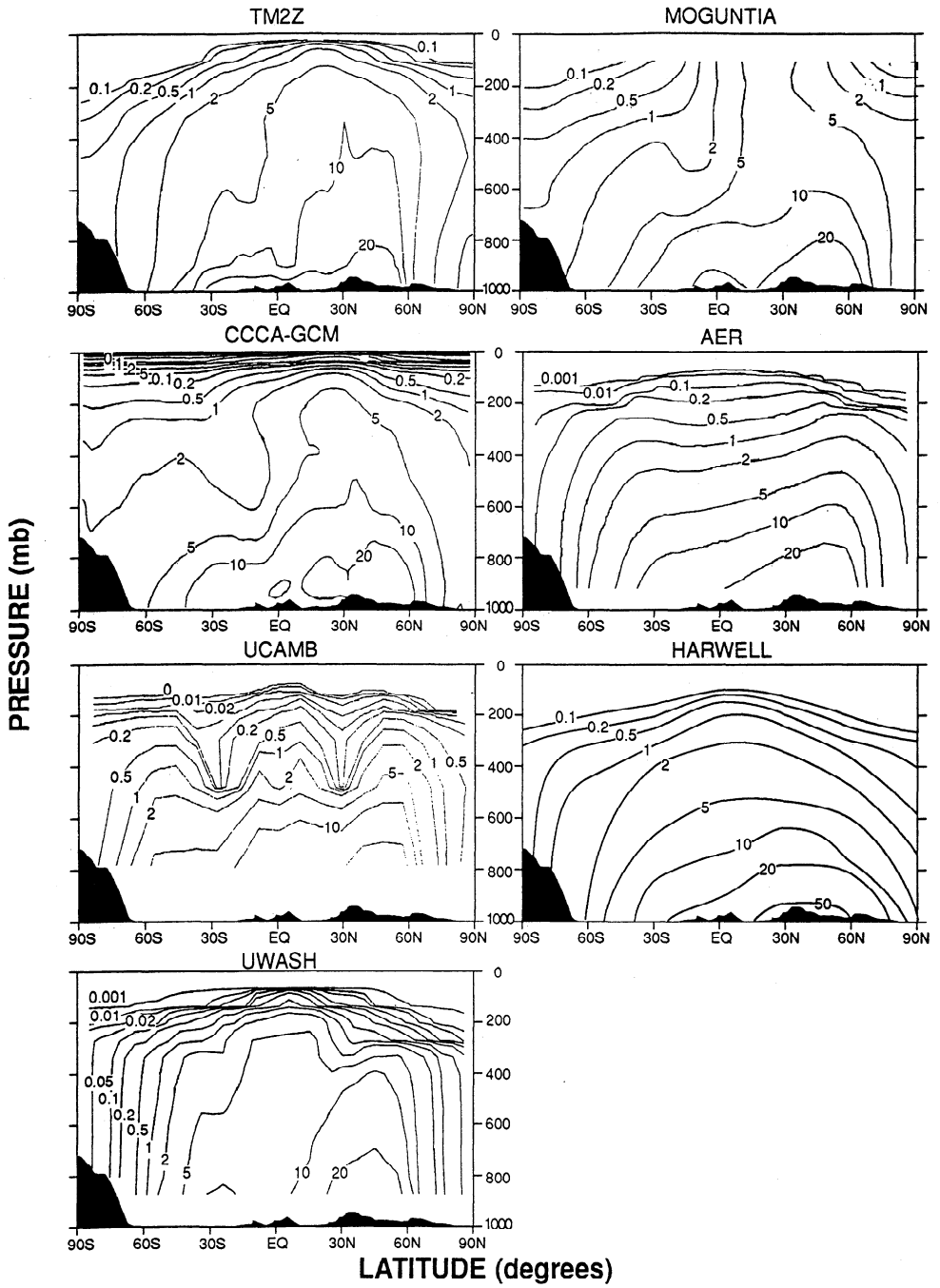

Figure 5. (continued)

tion is ~265 km. Vertical resolution is 11 levels up to 10 hPa, with 6-7 in the troposphere. Vertical transport by dry and moist convective processes is parameterized in terms of a Richardson number diffusion. The model has been used in many tracer transport studies [*Mahlman and Moxim*, 1978; *Levy et al.*, 1985; *Levy and Moxim*, 1989; *Kasibhatla et al.*, 1991, 1993].

D. GISS/H/I

This three-dimensional tracer model uses 4-hour time-average meteorological fields from the GISS GCM 2 [*Hansen et al.*, 1983]. Horizontal resolution is 4° latitude x 5° longitude. Vertical resolution is 9 layers up to 10 hPa, with 7-8 in the troposphere. Convective mass fluxes are diagnosed from the GCM. Advection is computed with the *Prather* [1986] scheme. The model has been used in many studies of tropospheric transport and chemistry [e.g., *Prather et al.*, 1987; *Jacob et al.*, 1987, 1993; *Spivakovsky et al.*, 1990; *Chin and Jacob*, 1996; *Koch et al.*, 1996] including simulations of ^{222}Rn [*Balkanski and Jacob*, 1990; *Jacob and Prather*, 1990; *Balkanski et al.*, 1992].

E. KNMI-TM2

This three-dimensional tracer model is based on the TM2 model of *Heimann* [1996] and the GISS GCM 2 [*Hansen et al.*, 1983]. Meteorological information is from the European Center for Medium-Range Weather Forecasting (ECMWF) forecast model (June-August 1989 and December-February 1990 in the present application). The ECMWF data are analyzed at 14 standard pressure levels (1000, 850, 700, 500, 400, 300, 250, 200,

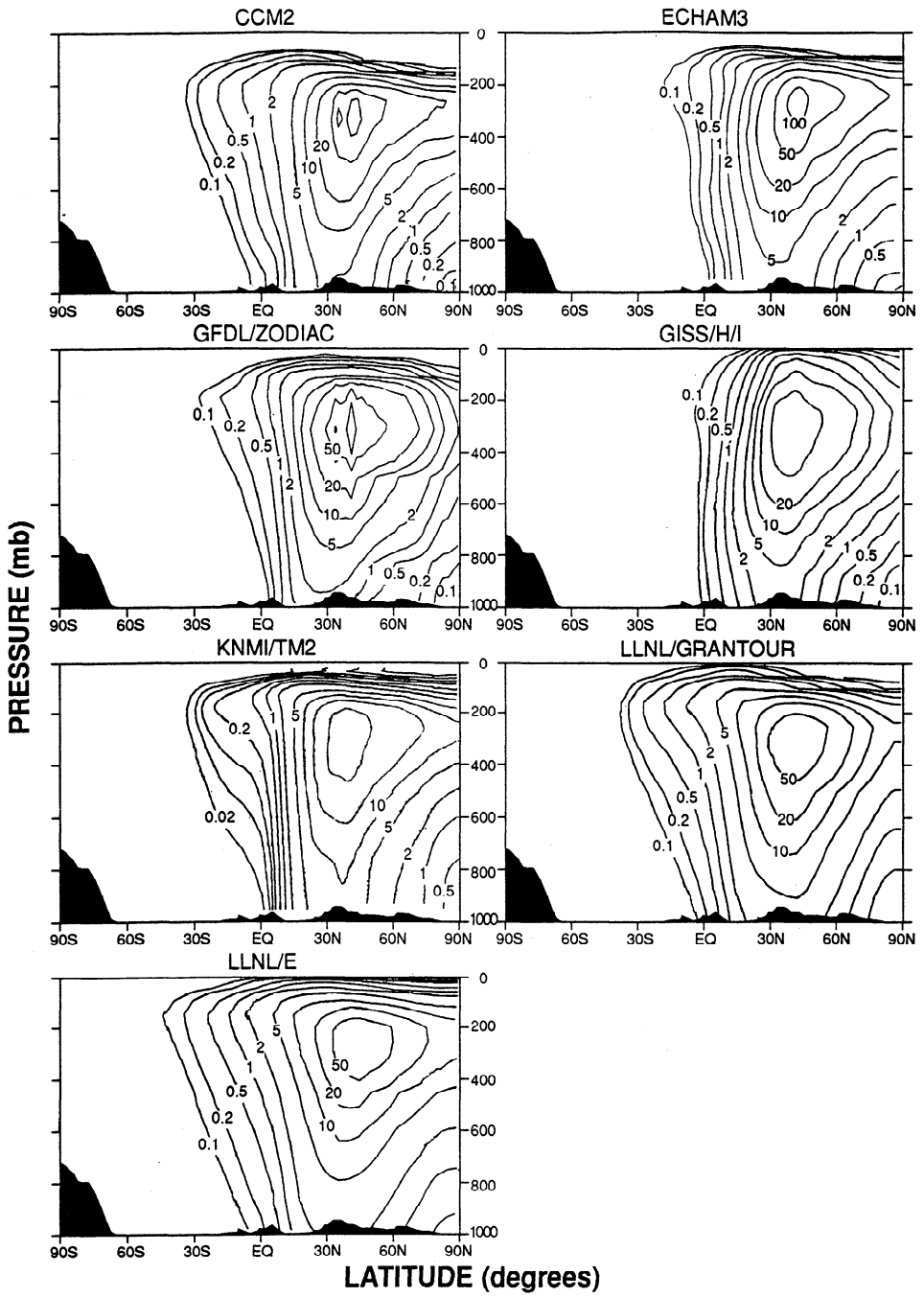

Figure 6. Zonal mean concentrations simulated by the different models in June-August for the aircraft tracer released in the upper troposphere at northern midlatitudes (case B). Units are 1×10^{-21} mol/mol.

150, 100, 70, 50, 30, and 10 hPa) on a horizontal scale of 2.5° x 2.5° and with a time frequency of 12 hours. The transport model has a resolution of 5°x4° and 15 σ levels in the vertical (up to 30 km altitude). Advection of trace gases is calculated by the slopes scheme of *Russell and Lerner* [1981] modified to avoid negative concentrations. Cumulus convection is parameterized following *Tiedtke* [1989]. Turbulent transport in the boundary layer is parameterized using the Richardson number [*Louis*, 1979] obtained from the ECMWF data.

F. LLNL/GRANTOUR

This three-dimensional tracer model [*Walton et al.*, 1988] uses 12-hour time average meteorological fields from the NCAR CCM1 GCM [*Williamson et al.*, 1987]. Resolution is 50,000 constant-mass air parcels whose dimensions average 100 hPa x 330 km x 330 km. Parcel information is periodically mapped to the CCM1 grid which has resolution of 4.4° latitude x 7.5° longitude x 12 vertical layers up to 10 hPa with 8-9 layers in the troposphere. Convective mass fluxes are diagnosed from the CCM1 GCM. Advection is by a nondiffusive Lagrangian scheme. Mixing ratio changes due to both diffusion and convection are calculated on the CCM1 fixed grid and then mapped to the parcels. The model has been used in many tropospheric chemistry studies [e.g., *Ghan et al.*, 1988; *Erickson et al.*, 1991; *Penner et al.*, 1991ab, 1993, 1994]. The simulations reported here are fully documented by *Dignon* [1993].

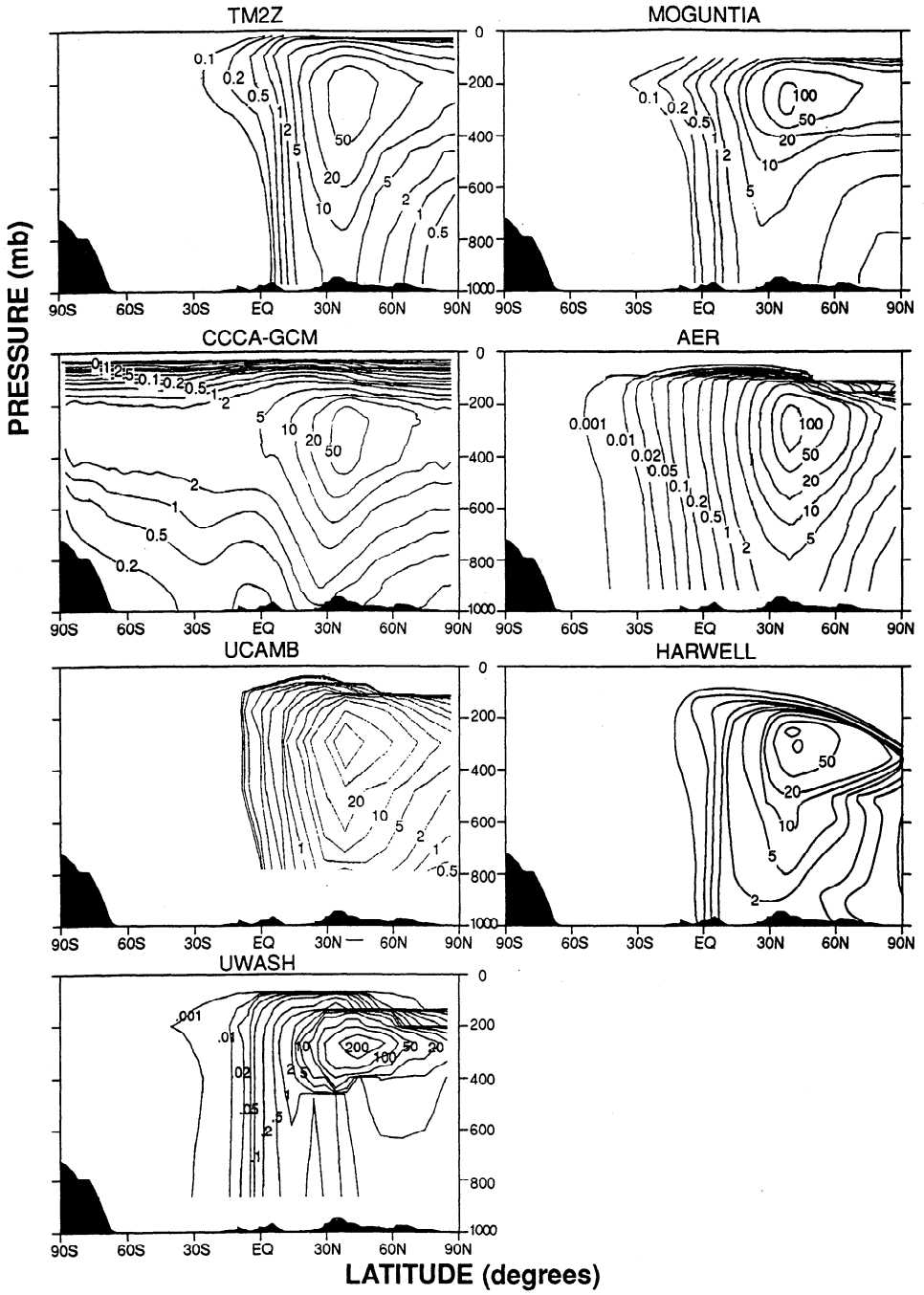

Figure 6. (continued)

G. LLNL/E

This three-dimensional model is identical with the LLNL/GRANTOUR except that the atmosphere is discretized by the Eulerian grid used in the CCM1 (no constant-mass air parcels are used). A second-order diffusion-limited Van Leer advection scheme is used. Diffusion and convection are included. The simulations reported here are fully documented by *Bergmann et al.* [1994].

H. LMD

This GCM is from the Laboratoire de Météorologie Dynamique (Centre National de la Recherche Scientifique) [*Sadourny and Laval*, 1984]. Horizontal grid is linear in longitude (5.6° resolution) and in sine of latitude (3.6° mean resolution). Vertical resolution is four levels in the boundary layer, four in the free troposphere, and three in the stratosphere. GCM-triggered dry and moist convection induces uniform vertical tracer mixing within the unstable layers and over a GCM-selected fraction of the column horizontal section. Vertical tracer diffusion in the boundary layer is parameterized using GCM-calculated diffusion coefficients. The model is fully described in two studies of ^{222}Rn, ^{210}Pb, and other tracers [*Genthon and Armengaud*, 1995a, b].

I. TM2Z

This three-dimensional tracer model uses 12-hour instantaneous meteorological fields analyzed by the ECMWF for the year 1990. The model is a new version of the TM1 model developed

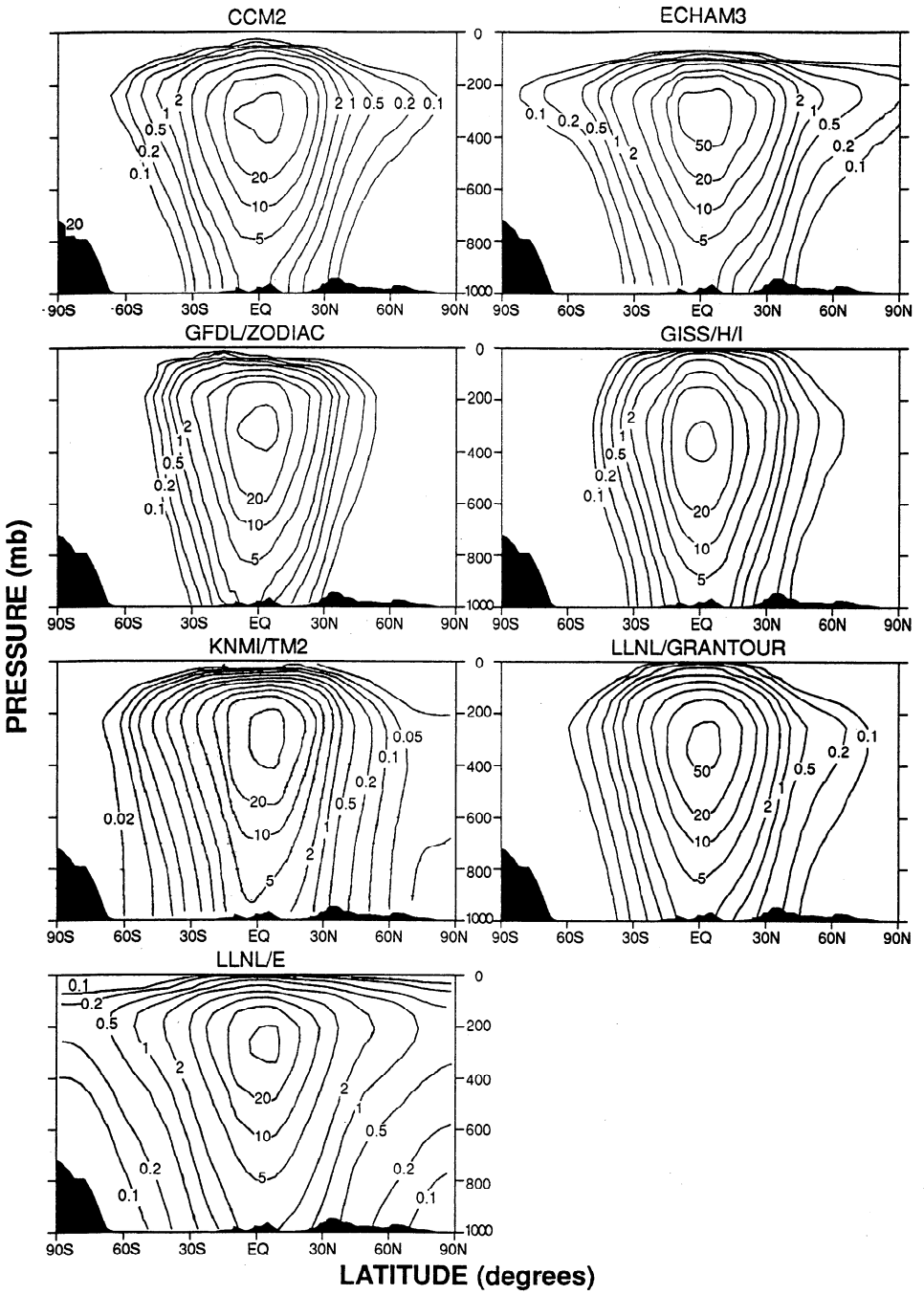

Figure 7. Zonal mean concentrations simulated by the different models in December-February for the tropical lightning tracer released in the upper troposphere (case C). Units are $1x10^{-21}$ mol/mol.

by *Heimann and Keeling* [1989] . Horizontal resolution is 2.5° x 2.5°. Vertical resolution is nine layers up to 10 hPa, with seven to eight layers in the troposphere. Convective mass fluxes are calculated following *Tiedtke* [1989] . Turbulent vertical transport is calculated based on the stability of the air using the scheme of *Louis* [1979] . The implementation of these schemes in the transport model is described by *Heimann* [1994] . The TM2Z model has been used to simulate ^{222}Rn and CO_2 concentrations [*Ramonet*, 1994; *Ramonet et al.*, 1996].

J. MOGUNTIA

This three-dimensional tracer model [*Zimmermann*, 1988; *Zimmermann et al.*, 1989] has a grid resolution of 10° x 10° x 100 hPa. The large-scale transport is based on observed monthly mean temperature and wind fields. Turbulent diffusion is parameterized proportional to the day-by-day deviation of the winds. Deep convection is performed explicitly according to observational occurrence of cumulus clouds [*Feichter and Crutzen*, 1990].

k. CCC-GCM

This second-generation GCM [*McFarlane et al.*, 1992] produces dynamical and tracer fields every 15 min. The model uses spectral transport with a horizontal resolution of 32 wavenumbers and a vertical resolution of ten levels up to 10 hPa, with six to seven levels in the troposphere. Convective transport and plane-

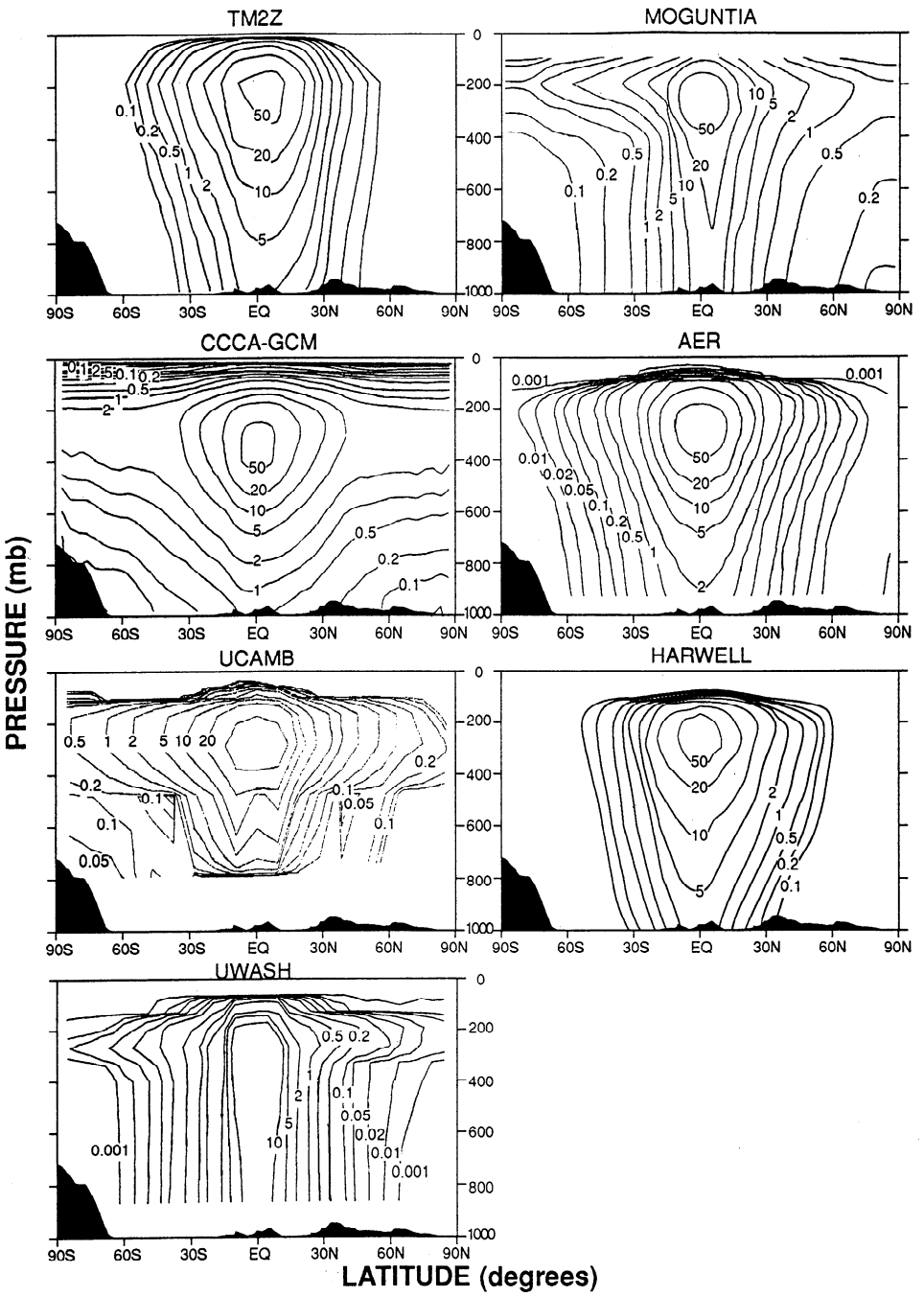

Figure 7. (continued)

tary boundary layer (PBL) mixing are parameterized. The convective tracer transport occurs for moist and dry events using a diffusive mixing associated with the convective adjustment scheme of the model. The degree of mixing is dependent upon the local strength of the convective column instability. The GCM was modified to include chemical tracers in a developmental form.

m. LaRC

This GCM has a σ coordinate, quasi-spectral, primitive equation formulation [*Grose et al.*, 1987; *Pierce et al.*, 1993]. Vertical resolution is 34 levels up to 95 km altitude, spaced about 100 hPa apart up to 200 hPa. A semi-implicit integration technique is used with a 15-min time step. A biharmonic diffusion is applied to the vorticity, divergence, and temperature prognostics. A surface drag proportional to wind speed is applied in the lowest model level. Vertical diffusion of momentum and temperature are incorporated via a nonlinear, time-split technique.

n. LLNL/IMPACT

This three-dimensional tracer model uses 6-hour meteorological fields from the tropospheric data assimilation model of the Data Assimilation Office at NASA Goddard. Horizontal resolution is 2° x 2.5°. Vertical resolution is 20 layers up to 10 hPa. At the time of this simulation the model was very much under development; most important, it did not have a convective transport mechanism. LLNL/IMPACT has since undergone upgrades, including the incorporation of a subgrid convection scheme.

o. MRI

This three-dimensional semi-Lagrangian tracer model uses 2-hourly meteorological fields from the MRI GCM [*Shibata and Chiba*, 1990]. Spectral horizontal resolution is R24 and vertical resolution is 23 levels up to 0.05 hPa. Vertical mixing of tracers in the PBL is parameterized following *Louis* [1979]. Convective transport is not included.

p. TOMCAT

This three-dimensional tracer model uses 6-hourly meteorological fields from the UGAMP GCM (see model q). Horizontal resolution is 2.8° latitude x 2.8° longitude. Vertical resolution is 19 levels up to 10 hPa. Tracer transport is performed using the second-order moments scheme of *Prather* [1986]. TOMCAT was developed at Météo France, Toulouse and University of Cambridge. The model has been used in many stratospheric chemistry studies [e.g., *Chipperfield et al.*, 1993, 1994, 1995] and is being developed for tropospheric studies. The experiments described in this paper did not include any tracer transport other than advection. Since the WCRP workshop treatments of convection [*Tiedtke*, 1989] and vertical turbulent diffusion [*Louis*, 1979] have been added to the model.

q. UGAMP

This GCM is derived from cycle 27 of the ECMWF model [*European Center for Medium Range Weather Forecasting (ECMWF)*, 1988]. Spectral horizontal resolution is T42 [*Simmons et al.*, 1988]. Chemical tendencies and parameterized physical processes are resolved on a 2.8° x 2.8° Gaussian grid [*Tiedtke et al.*, 1988]. Vertical resolution is 19 hybrid levels up to 10 hPa. The planetary boundary layer is modeled explicitly by using five model levels and a 30-min time step. Vertical advection is computed with a fourth-order total variation diminishing (TVD) algorithm [*Thuburn*, 1993]. The convective adjustment scheme for moisture is from *Betts* (1986); *Betts and Miller* [1993]. There is no convective transport of tracers.

R. AER

This two-dimensional model uses the diabatic circulation based on calculated heating rates and horizontal eddy diffusion coefficients function of latitude, altitude, and season. Horizontal resolution: 9.5°. Vertical resolution is ~3.5 km up to 60 km. The model has been used in many stratospheric chemistry studies [e.g., *Ko et al.*, 1984, 1985, 1986, 1989, 1991; *Sze et al.*, 1989; *Rodriguez et al.*, 1991; *Weisenstein et al.*, 1991, 1992; *Plumb and Ko*, 1992].

S. UCAMB

This classical Eulerian two-dimensional model uses specified eddy diffusion coefficients and calculated mean circulation, based on forcing by latent and radiative heating and eddy transport processes. Horizontal resolution is 9.5° and vertical resolution is ~3.5 km up to 60-km. A full description of the model is given by *Harwood and Pyle* [1980] and *Law and Pyle* [1993]. The model has been used in tropospheric chemistry studies [e.g., *Law and Pyle*, 1993; *Bekki et al.*, 1994].

T. HARWELL

This two-dimensional model has 12 vertical layers, each of 2 km height, and 24 equal-area latitudinal bands. It uses circulation derived by *Plumb and Mahlman* [1987]. The simulation of transport has been tested with the atmospheric tracers ^{85}Kr, $CFCl_3$, CF_2Cl_2 [*Hough*, 1989], and with the inclusion of a chemical mechanism, the reactive species CH_4, CO, nonmethane hydrocarbons, O_3, peroxyacetylnitrate (PAN), and peroxides [*Hough*, 1991; *Hough and Derwent*, 1990; *Hough and Johnson*, 1991; *Johnson et al.*, 1992].

U. UW

This two-dimensional model was developed by *Tung* [1982, 1986] *Yang et al.* [1990, 1991] and *Olaguer et al.* [1992]. It is formulated in isentropic coordinates. Horizontal resolution: 10°. Vertical resolution is 48 levels from 0 to 54 km, including 8 below 100 hPa. Transport parameters are derived from observed 1980 atmospheric temperatures. The model has been validated using tracers which are sensitive to tropospheric transport and chemical parameters (^{85}Kr, CFC-11, CFC-12, and methylchloroform [*Brown*, 1993]). The distribution of ^{222}Rn in the troposphere is sensitive to the vertical diffusion parameter K_{zz}, specified here as 50 m^2 s^{-1} in the tropics and 10 m^2 s^{-1} at higher latitudes. These values are the same as those used by *Brown* [1993] and are consistent with results from *Plumb and McConalogue* [1988] and *Plumb and Mahlman* [1987].

Acknowledgements. The intercomparison workshop was sponsored by the World Climate Research Program with V. Savchenko as project manager. D.J. Jacob thanks G.M. Gardner for conducting the GISS/H/I simulations and acknowledges support from NASA-NAG5-2688 and NASA-NAGW-2632. P. Kasibhatla acknowledges support from NASA-NAGW-3770. D.J. Bergmann acknowledges John Walton for developing the Lagrangian version of the LLNL model and guiding him in the development of the Eulerian version. C. Genthon thanks the Laboratoire de Météorologie Dynamique (CNRS, Paris) for granting rights to use and modify their GCM, and the Centre Grenoblois de Calcul Vectoriel for allocating computer time. Y.J. Balkanski and M. Ramonet thank P. Bousquet and P. Monfray for simulations with TM2Z, express gratitude to M. Heimann who developed the TM2 code, and acknowledge computing support from the Commissariat à l'Energie Atomique/LMCE and IDRIS. P. Zimmermann acknowledges support from BMBF grant 07KFT52-4 for development of the MOGUNTIA model at the Max-Planck-Institut für Chemie (Mainz) under EUROTRAC/GLOMAC. S.R. Beagley and J. de Grandpré thank the Canadian Climate Centre (CCC) for the use of the CCC-GCM by York University. M. Chipperfield thanks P. Simon and M. Heimann for their assistance. M. Chipperfield, Z. Stockwell, K.S. Law, O. Wild, and C.E. Reeves thank the U.K. DOE and UGAMP for funding. H. Yang acknowledges support from NASA-NAG-1-1404, and M. Brown acknowledges support from DOE NIGEC under grant W/GEC 93-013.

References

Allen, D. J, R. B. Rood, A. M. Thompson, and R. D. Hudson, Three-dimensional Rn 222 calculations using assimilated meteorological data and a convective mixing algorithm, *J. Geophys. Res., 101*, 6871-6882, 1996.

Balkanski, Y. J., and D. J. Jacob, Transport of continental air to the subantarctic Indian Ocean, *Tellus Ser. B, 42*, 62-75, 1990.

Balkanski, Y. J., D. J. Jacob, R. Arimoto, and M. A. Kritz, Long-range transport of radon-222 over the North Pacific Ocean: Implications for continental influence, *J. Atmos. Chem., 14*, 353-374, 1992.

Balkanski, Y. J., D. J. Jacob, G. M. Gardner, W. M. Graustein, and K. K. Turekian, Transport and residence times of continental aerosols inferred from a global three-dimensional simulation of ^{210}Pb, *J. Geophys. Res., 98*, 20,573-20,586, 1993.

Bekki, S., K. S. Law, and J. A. Pyle, Effect of ozone depletion on atmospheric CH_4 and CO concentrations, *Nature, 371*, 595-597, 1994.

Bergmann, D., J. Dignon, J. Penner, and J. Walton, Results from the LLNL Eulerian GRANTOUR model for the World Climate Research Program 1993 Workshop on the Parameterization of Sub-Grid Scale Tracer Transport, *LLNL Rep. UCRL-ID 116544*, Lawrence Livermore Nat. Lab., Livermore, Calif., 1994.

Betts, A. K., A new convective adjustment scheme, I, Observational and theoretical basis, *Q. J. R. Meteorol. Soc., 112*, 677-691, 1986.

Betts, A. K., and M. J. Miller, The Betts-Miller scheme, in *The Representation of Cumulus Convection in Numerical Models of the Atmosphere*, edited by K. Emmanuel and D. Raymond, Am. Meteorol. Soc., Boston, Mass., 1993.

Brost, R. A. and R. B. Chatfield, Transport of radon in a three-dimensional, subhemispheric model, *J. Geophys. Res., 94*, 5095-5120, 1989.

Brost R. A., J. Feichter, and M. Heimann, Three-dimensional simulation of ^{7}Be in a global climate model, *J. Geophys. Res., 96,* 22,423-22,445, 1991.

Brown, M., Deduction of emissions of source gases using an objective inversion algorithm and a chemical transport model, *J. Geophys. Res., 98,* 12,639-12,660, 1993.

Cess, R.D., et al., Intercomparison and interpretation of climate feedback processes in 19 atmospheric general circulation models, *J. Geophys. Res., 95,* 16,601-16,615, 1990.

Cubasch, U., K. Hasselmann, H. Hoeck, E. Maier-Reimer, U. Mikolajewicz, B. D. Santer, and R. Sausen, Time-dependent greenhouse warming computations with a coupled ocean-atmosphere model, *Clim. Dyn., 8,* 55-69, 1992.

Chin, M., and D. J. Jacob, Anthropogenic and natural contributions to atmospheric sulfate: a global model analysis, *J. Geophys. Res., 101,* 18,691-18,699, 1996.

Chipperfield, M. P., D. Cariolle, P. Simon, R. Ramaroson, and D. J. Lary, A three-dimensional modeling study of trace species in the Arctic lower stratosphere during winter 1989-1990, *J. Geophys. Res., 98,* 7199-7218, 1993.

Chipperfield, M.P., D. Cariolle, and P.Simon, A three-dimensional chemical transport model study of chlorine activation during EASOE, *Geophys. Res. Lett., 21,* 1467-1470, 1994.

Chipperfield, M.P., J.A. Pyle, C.E. Blom, N. Glatthor, M. Hopfner, T. Gulde, C. Piesch, and P. Simon, The Variability of $ClONO_2$ and HNO_3 in the Arctic polar vortex: Comparison of Transall MIPAS measurements and three-dimensional model results, *J. Geophys. Res., 100,* 9115-9129, 1995.

Dignon, J., Results from the LLNL GRANTOUR model for the World Climate Research Program 1993 Workshop on the Parameterization of Sub-Grid Scale Tracer Transport, *LLNL Rep. UCRL-ID 116544,* Lawrence Livermore Nat. Lab., Livermore, Calif., 1994.

Dörr, H., and K. O. Munnich, ^{222}Rn flux and soil air concentration profiles in West Germany. Soil ^{222}Rn as a tracer for gas transport in the unsaturated soil zone, *Tellus, Ser. B, 42,* 20-28, 1990.

Erickson, D. J., III, J. J. Walton, S. J. Ghan, and J. E. Penner, Three-dimensional modeling of the global atmospheric sulfur cycle: A first step, *Atmos. Environ., 25A,* 2513-2520, 1991.

European Centre for Medium-Range Weather Forecasting (ECMWF), *Res. Manual 2,* ECMWF forecast models adiabatic part, ECMWF Res. Dep., Reading, England, 1988.

Feichter, J., and P.J. Crutzen, Parameterization of vertical tracer transport due to deep cumulus convection and its evaluation with $^{222}Radon$ measurements, *Tellus, 42, Ser. B,* 100-117, 1990.

Feichter, J., R. A. Brost, and M. Heimann, Three-dimensional modeling of the concentration and deposition of ^{210}Pb aerosols, *J. Geophys. Res., 96,* 22,447-22,469, 1991a.

Feichter, J., E. Roeckner, U. Schlese, and M. Windelband, Tracer transport in the Hamburg climate model, in *Air Pollution Modeling and Its Applications VIII,* edited by H. van Dop and D. G. Steyn, Plenum, New York, 1991b.

Feichter J., E. Kjellström, H. Rodhe, F. Dentener, J. Lelieveld, and G.-J Roelofs, Simulation of the tropospheric sulfur cycle in a global climate model, *Atmos. Environ., 30,* 1693-1708, 1996.

Fukuda, K., and S. Tsunogai, Pb-210 in precipitation in Japan and its implication for the transport of continental aerosols across the ocean, *Tellus, 27,* 514-521, 1975.

Genthon, C., and A. Armengaud, Radon 222 as a comparative tracer of transport and mixing in two general circulation models of the atmosphere, *J. Geophys. Res., 100,* 2849-2866, 1995a.

Genthon, C., and A. Armengaud, GCM simulations of atmospheric tracers in the polar regions: South Pole (Antarctica) and Summit (Greenland) cases, *Sci. Total Environ., 160/161,* 101-116, 1995b.

Gesell, T.F., Background atmospheric ^{222}Rn concentrations outdoors and indoors: A review, *Health Phys., 45,* 289-302, 1983.

Ghan, S.J., M.C. MacCracken, and J.J. Walton, Climatic response to large atmospheric smoke injections: Sensitivity studies with a tropospheric general circulation model, *J. Geophys. Res., 93,* 8315-8337, 1988.

Gold, S., H. Barkhau, W. Shleien, and B. Kahn, Measurement of naturally occurring radionuclides in air, in *The Natural Radiation Environment,* edited by J.A.S. Adams and W.M. Lowder, pp. 369-382, Univ. of Chicago Press, Chicago, Ill., 1964.

Graustein, W. C., and K. K. Turekian, Radon fluxes from soils to the atmosphere measured by ^{210}Pb- ^{226}Ra disequilibrium in soils, *Geophys. Res. Lett., 17,* 841-844, 1990.

Grose, W. L., J. E. Nealy, R. E. Turner, and W. T. Blackshear, Modeling the transport of chemically active constituents in the stratosphere, in *Transport Processes in the Middle Atmosphere,* edited by G. Visconti, 485 pp., D. Reidel, Norwell, Mass., 1987.

Hack, J. J., Parameterization of moist convection in the NCAR Community Climate Model, CCM2, *J. Geophys. Res., 98,* 5551-5568, 1993.

Hack, J. J., B. A. Boville, B. P. Briegleb, J. T. Kiehl, P. J. Rasch, and D. L. Williamson, Description of the NCAR Community, Climate Model (CCM2), *NCAR Tech. Note, NCAR/TN--382+STR,* 108 pp., Natl. Cent. for Atmospheric Res., Boulder, Colo., 1993.

Hack, J.J., B.A. Boville, J.T. Kiehl, P.J. Rasch, and D.L. Williamson, Climate statistics from the NCAR Community Climate Model CCM2, *J. Geophys. Res., 99,* 20,785-20,813, 1994.

Hansen, J., G. Russell, D. Rind, P. Stone, A. Lacis, S. Lebedeff, R. Ruedy, and L. Travis, Efficient three-dimensional global models for climate studies: Models I and II, *Mon. Weather Rev., 111,* 609-662, 1983.

Hartley, D., D.L. Williamson, P.J. Rasch, and R. Prinn, Examination of tracer transport in the NCAR CCM2 by comparison of $CFCl_3$ simulations with ALE/GAGE observations, *J. Geophys. Res., 99,* 12,885-12,896, 1994.

Harwood, R.S., and J.A. Pyle, The dynamical behavior of a two-dimensional model of the stratosphere, *Q. J. R. Meteorol. Soc., 106,* 395-420, 1980.

Heimann, M., *The Global Atmospheric Tracer Model TM2: Model Description and User Manual,* Max-Planck-Inst. für Meteorol., Hamburg, Germany, 1994.

Heimann, M., and C.D. Keeling, A three-dimensional transport model for atmospheric CO_2, 2, Model description and simulated tracer experiments, *Tech. Rep. 33,* 105 pp., Max-Planck-Inst. für Meteorol., Hamburg, Germany, 1989.

Heimann, M., P. Monfray, and G. Polian, Modeling the long-range transport of ^{222}Rn to subantarctic and antarctic areas, *Tellus, Ser. B., 42,* 83-99, 1990.

Holtslag, A. A. M., and B. A. Boville, Local versus non-local boundary-layer diffusion in a global climate model, *J. Clim., 6,* 1825--1842, 1993.

Hough, A. M., The development of a two-dimensional global tropospheric model, 1, The model transport, *Atmos. Environ., 23,* 1235-1261, 1989.

Hough, A. M., Development of a two-dimensional global tropospheric model: Model chemistry, *J. Geophys. Res., 96,* 7325-7362, 1991.

Hough, A. M., and R.G. Derwent, Changes in the global concentration of tropospheric ozone due to human activities, *Nature, 344,* 645-650, 1990.

Hough, A. M., and C.E. Johnson, Modelling the role of nitrogen oxides, hydrocarbons and carbon monoxide in the global formation of tropospheric oxidants, *Atmos. Environ., 25,* 1819-1835, 1991.

Jacob, D. J., and M. J. Prather, Radon-222 as a test of boundary layer convection in a general circulation model, *Tellus, Ser. B., 42,* 118-134, 1990.

Jacob, D. J., M. J. Prather, S. C. Wofsy, and M. B. McElroy, Atmospheric distribution of ^{85}Kr simulated with a general circulation model, *J. Geopyhys. Res., 92,* 6614-6626, 1987.

Jacob, D. J., et al., Simulation of summertime ozone over North America, *J. Geophys. Res., 98,* 14,797-14,816, 1993.

Johnson, C., J. Henshaw, and G. McInnes, Impact of aircraft and surface emissions of nitrogen oxides on tropospheric ozone and global warming, *Nature, 355,* 69-71, 1992.

Kasibhatla, P. S., H. Levy, W. J. Moxim, and W. L. Chameides, The relative importance of stratospheric photochemical production on tropospheric NOy levels: A model study, *J. Geophys. Res., 96,* 18,631-18,646, 1991.

Kasibhatla, P.S., H. Levy II, and W.J. Moxim, Global NOx, HNO_3, PAN, and NOy distributions from fossil-fuel combustion emissions: A model study, *J. Geophys. Res., 98,* 7165-7181, 1993.

Ko, M.K. W., N. D. Sze, M. Livshits, M. B. McElroy, and J. A. Pyle, The seasonal and latitudinal behavior of trace gases and O_3 as simulated by a two-dimensional model of the atmosphere, *J. Atmos. Sci., 41,* 2381-2408, 1984.

Ko, M. K. W., K. K. Tung, D. K. Weisenstein, and N. D. Sze, A zonal mean model of stratospheric tracer transport in isentropic coordinates: Numerical simulation for nitrous oxide and nitric acid, *J. Geophys. Res., 90,* 2313-2329, 1985.

Ko, M. K. W., M. B. McElroy, D. K. Weisenstein, and N. D. Sze, Lightning: A possible source of stratospheric odd nitrogen, *J. Geophys. Res., 91,* 5395-5404, 1986.

Ko, M. K. W., N. D. Sze, and D. K. Weisenstein, The roles of dynamical and chemical processes in determining the stratospheric concentration

of ozone in one-dimensional and two-dimensional models, *J. Geophys. Res., 94,* 9889-9896, 1989.

Ko, M. K. W., N. D. Sze, and D. K. Weisenstein, Use of satellite data to constrain model-calculated atmospheric lifetimes for N_2O: Implications for other trace gases, *J. Geophys. Res., 96,* 7547-7552, 1991.

Koch, D. M., D. J. Jacob, and W. C. Graustein, Vertical transport of tropospheric aerosols as indicated by ^{7}Be and ^{210}Pb in a chemical tracer model, *J. Geophys. Res., 101,* 18,651-18,666, 1996.

Kritz, M. A., J.-C. Le Roulley, and E. F. Danielsen, The China Clipper. Fast advective transport of radon rich air from the Asian boundary layer to the upper troposphere near California, *Tellus, Ser. B., 42,* 46-61, 1990.

Lambert, G., G. Polian, and D. Taupin, Existence of periodicity in radon concentrations and the large-scale circulation at latitudes between 40° and 70° south, *J. Geophys. Res., 75,* 2341-2345, 1970.

Lambert, G., G. Polian, J. Sanak, B. Ardouin, A. Buisson, A. Jegou, and J. C. Leroulley, Cycle du radon et de ses descendants: Application à l'étude des échanges troposphère-stratosphère, *Ann. Geophys., 38,* 497-531, 1982.

Lambert, G., G. Polian, B. Ardouin, J. Renault, and Y. Balkanski, *CFR Database of ^{222}Rn, ^{220}Rn, and ^{210}Pb in Subantarctic and Antarctic Atmosphere*, Centre des Faibles Radioactiv., Gif-sur-Yvette, France, 1995. (Correspondence concerning this database should be sent to Y. J. Balkanski.)

Law, K. S., and J. A. Pyle, Modelling budgets of tropospheric trace gases, 1, Ozone and odd nitrogen, *J. Geophys. Res., 98,* 18,377-18,400, 1993.

Levy, H., II, and W. J. Moxim, Simulated global distribution and deposition of reactive nitrogen emitted by fossil fuel combustion, *Tellus, 41,* 256-271, 1989.

Levy, H., II, J. D. Mahlman, W. J. Moxim, and S. C. Liu, Tropospheric ozone: The role of transport, *J. Geophys. Res., 90,* 3753-3772, 1985.

Liu, S. C., J. R. McAfee, and R. J. Cicerone, Radon 222 and tropospheric vertical transport, *J. Geophys. Res., 89,* 7291-7297, 1984.

Louis, J. F., A parametric model of vertical eddy fluxes in the atmosphere, *Boundary Layer Meteorol., 17,* 187-202, 1979.

Mahlman, J. D., and W. J. Moxim, Tracer simulation using a general circulation model: Results from a midlatitude source experiment, *J. Atmos. Sci., 35,* 1340-1374, 1978.

Mahowald, N. M., P. J. Rasch, and R. G. Prinn, Cumulus parameterizations in chemical transport models, *J. Geophys. Res., 100,* 26173-26190, 1995.

Manabe, S., D. G. Hahn, and J. L. Holloway Jr., The seasonal variation of the tropical circulation as simulated by a global model of the atmosphere, *J. Atmos. Sci., 31,* 43-83, 1974.

McFarlane, N. A., G. J. Boer, J.-P. Blanchet, and M. Lazare, The Canadian Climate Centre second generation GCM and its equilibrium climate, *J. Clim., 5,* 1013-1044, 1992.

Miller, J. M., J. L. Moody, J. M. Harris, and A. Gaudry, A 10-year trajectory flow climatology for Amsterdam Island, 1980-1989, *Atmos. Environ., 27A,* 1909-1916, 1993.

Nazaroff, W. W., Radon transport from soil to air, *Rev. Geophys., 30,* 137-160, 1992.

Nazarov, L. E., A. F. Kuzenkov, S. G. Malakhov, L. A. Volokitina, Y. I. Gasiyev, and A. S. Vasil'yev, Radioactive aerosol distribution in the middle and upper troposphere over the USSR in 1963-1968, *J. Geophys. Res., 75,* 3575-3588, 1970.

Olaguer, E. P., H. Yang, and K. K. Tung, A reexamination of the radiative balance of the stratosphere, *J. Atmos. Sci., 49,* 1242-1263, 1992.

Penner, J. E., C. S. Atherton, J. Dignon, S. J. Ghan, J. J. Walton, and S. Hameed, Tropospheric nitrogen: A three-dimensional study of sources, distribution, and deposition, *J. Geophys. Res., 96,* 959-990, 1991a.

Penner, J. E., S. J. Ghan, and J. J. Walton, The role of biomass burning in the budget and cycle of carbonaceous soot aerosols and their climate impact, in *Global Biomass Burning,* edited by J. Levine, pp. 387-393, MIT press, Cambridge, Mass., 1991b.

Penner, J. E., H. Eddleman, and T. Novakov, Towards the development of a global inventory of black carbon emissions, *Atmos. Environ., 27A,* 1277-1295, 1993.

Penner, J. E., C. A. Atherton, and T. Graedel, Global emissions and models of photochemically active compounds, in *Global Atmospheric-Biospheric Chemistry*, edited by R. Prinn, pp. 223-248, Plenum, New York, 1994.

Pierce, R. B., W. T. Blackshear, T. D. Fairlie, W. L. Grose, and R. E. Turner, The interaction of radiative and dynamical processes during a simulated sudden stratospheric warming, *J. Atmos. Sci., 50,* 3829-3851, 1993.

Plumb, R. A., and M. K. W. Ko, Interrelationships between mixing ratios of long-lived stratospheric constituents, *J. Geophys. Res., 97,* 10,145-10,156, 1992.

Plumb, R. A., and J. D. Mahlman, The zonally-averaged transport characteristics of the GFDL general circulation/transport model, *J. Atmos. Sci., 44,* 298-327, 1987.

Plumb, R. A., and D. D. McConalogue, On the meridional structure of long-lived tropospheric constituents, *J. Geophys. Res., 93,* 15,897-15,913, 1988.

Polian, G., G. Lambert, B. Ardouin, and A. Jegou, Long-range transport of radon in subantarctic and antarctic areas, *Tellus, Ser. B., 38,* 178-189, 1986.

Prather, M. J, Numerical advection by conservation of second-order moments, *J. Geophys. Res., 91,* 6671-6681, 1986.

Prather, M. J., M. B. McElroy, S. C. Wofsy, G. Russell, and D. Rind, Chemistry of the global troposphere: Fluorocarbons as tracers of air motion, *J. Geophys. Res., 92,* 6579-6613, 1987.

Preiss, N., M.-A. Mélières, and M. Pourchet, A compilation of data on lead 210 concentration in surface air and fluxes at the air-surface and water-sediment interfaces, *J. Geophys. Res.*, in press, 1996.

Ramonet M., Variabilité du CO_2 atmosphérique en régions australes: Comparaison modèle-mesures, diploma thesis, 295 pp., Univ. de Paris VII, 1994.

Ramonet M., J. C. Le Roulley, P. Bousquet, and P. Monfray, Radon-222 measurements during the TROPOZ II campaign and comparison with a global atmospheric transport model, *J. Atmos. Chem., 23,* 107-136, 1996.

Rasch, P., and D. Williamson, Computational aspects of moisture transport in global models of the atmosphere, *Q. J. R. Meteorol. Soc., 116,* 1071-1090, 1990.

Rasch, P. J., X. X. Tie, B. A. Boville, and D. L. Williamson, A three-dimensional transport model for the stratosphere, *J. Geophys. Res., 99,* 999-1018, 1994.

Rasch, P. J., B. A. Boville, and G. P. Brasseur, A three-dimensional general circulation model with coupled chemistry for the middle atmosphere, *J. Geophys. Res., 100,* 9041-9071, 1995.

Rind, D., and J. Lerner, Use of on-line tracers as a diagnostic tool in general circulation model development, 1, Horizontal and vertical transport in the troposphere, *J. Geophys. Res., 101,* 12,667-12,683, 1996.

Rodriguez, J. M., M. K. W. Ko, and N. D. Sze, Role of heterogeneous conversion of N_2O_5 on sulphate aerosols in global ozone losses, *Nature, 352,* 134-137, 1991.

Roeckner, E., et al., Simulation of the present-day climate with the ECHAM model: impact of model physics and resolution, *Tech. Rep. 93,* Max-Planck-Inst. für Meteorol., Hamburg, Germany, 1992.

Roeckner, E., T. Siebert and J. Feichter, Climatic response to anthropogenic sulfate forcing simulated with a general circulation model, in *Aerosol Forcing of Climate,*, edited by R. J. Charlson and J. Heintzenberg, pp. 349-362, John Wiley, New York, 1995.

Roelofs, G.-J., and J. Lelieveld, Distribution and budget of O_3 in the troposphere calculated with a chemistry-general circulation model, *J. Geophys. Res., 100,* 20,983-20,998, 1995.

Russell, G. L., and J. A. Lerner, A new finite-differencing scheme for the tracer transport equation, *J. Appl. Meteorol., 20,* 1483-1498, 1981.

Sadourny R., and K. Laval, January and July performances of the LMD-GCM, in *New Perspectives in Climate Modelling,* edited by A. L. Berger and C. Nicolis, pp. 173-197, Elsevier, New York, 1984.

Schery, S. D., S. Whittlestone, K. P. Hart, and S. E. Hill, The flux of radon and thoron from Australian soils, *J. Geophys. Res., 94,* 8567-8576, 1989.

Shibata, K., and M. Chiba, A simulation of seasonal variation of the stratospheric circulation with a general circulation model, *J. Meteorol. Soc. Jpn., 68,* 687-703, 1990.

Simmons, A., D. Burridge, M. Jarraud, C. Girard, and W. Wergen, The ECMWF medium-range prediction model: Development of the numerical formulations and the impact of increased resolution, *Meteorol. Atmos. Phys., 40,* 28-60, 1988.

Spivakovsky, C.M., R. Yevich, J.A. Logan, S.C. Wofsy, M.B. McElroy, and M.J. Prather, Tropospheric OH in a three-dimensional chemical tracer model: An assessment based on observations of CH_3CCl_3, *J. Geophys. Res., 95,* 18,441-18,472, 1990.

Sze, N. D., M. K. W. Ko, D. K. Weisenstein, J. M. Rodriguez, R. S. Stolarski, and M. R. Schoeberl, Antarctic ozone hole: Possible implications for ozone trends in the southern hemisphere, *J. Geophys. Res., 94,* 11,521-11,528, 1989.

Thuburn, J., Use of a flux-limited scheme for vertical advection in a GCM, *Q. J. R. Meteorol. Soc., 119*, 469-487, 1993.

Tiedtke, M., A comprehensive mass flux scheme for cumulus parameterization in large-scale models, *Mon. Weather Rev., 117*, 1779-1800, 1989.

Tiedtke, M., W. Heckley, and J. Slingo, Tropical forecasting at ECMWF: The influence of physical parametrization on the mean structure of forecasts and analyses, *Q. J. R. Meteorol. Soc., 114*, 639-664, 1988.

Tung, K. K., On the two-dimensional transport of stratospheric gases in isentropic coordinates, *J. Atmos. Sci., 39*, 2600-2618, 1982.

Tung, K. K., Nongeostrophic theory of zonally averaged circulation. Part I, Formulation, *J. Atmos. Sci., 43*, 2600-2618, 1986.

Turekian, K. K., Y. Nozaki, and L. K. Benninger, Geochemistry of atmospheric radon and radon products, *Annu. Rev. Earth Planet. Sci., 5*, 227-255, 1977.

Walton, J. J., M. C. MacCracken, and S. J. Ghan, A global-scale Lagrangian trace species model of transport, transformation, and removal processes, *J. Geophys. Res., 93*, 8339-8354, 1988.

Weisenstein, D. K., M. K. W. Ko, J. M. Rodriguez, and N. D. Sze, Impact of heterogeneous chemistry on model calculated ozone change due to high speed civil transport aircraft, *Geophys. Res. Lett., 18*, 1991-1994, 1991.

Weisenstein, D. K., M. K. W. Ko, and N. D. Sze, The chlorine budget of the present day atmosphere: A modeling study, *J. Geophys. Res., 97*, 2547-2559, 1992.

Wilkening, M. H., and W. E. Clements, Radon 222 from the ocean surface, *J. Geophys. Res., 80*, 3828-3830, 1975.

Wilkening, M.H., W.E. Clements, and D. Stanley, Radon 222 flux measurements in widely separated regions, in *The Natural Radiation Environment II*, pp. 717-730, U. S. Energy and Res. Dev. Admin., Oak Ridge, Tenn., 1975.

Williamson, D. L., J. T. Kiehl, V. Ramanathan, R. E. Dickinson, and J. J. Hack, Description of NCAR Community Climate Model (CCM1), *NCAR Tech. Note, NCAR/TN-285+STR*, Natl. Cent. for Atmos. Res., Boulder, Colo., 1987. (Available as *NTIS PB87-203782*, 112 pp., from Natl. Tech. Inf. Serv., Springfield, Va.)

Yang, H., K. K. Tung, and E. Olaguer, Nongeostrophic theory of zonally averaged circulation, Part II, Eliassen-Palm flux divergence and isentropic mixing coefficient, *J. Atmos. Sci., 47*, 215-241, 1990.

Yang, H., E., Olaguer, and K. K. Tung, Simulation of the present-day atmospheric ozone, odd nitrogen, chlorine and other species using a coupled two-dimensional model in isentropic coordinates, *J. Atmos. Sci., 48*, 442-471, 1991.

Zimmermann, P. H., MOGUNTIA: A handy global tracer model, in *Air Pollution Modeling and Its Applications VI*, edited by H. van Dop, pp. 593-608, Plenum, New York, 1988.

Zimmermann, P. H., H. Feichter, H. K. Rath, P. J. Crutzen, and W. Weiss, A global three-dimensional source-receptor model investigating ^{85}Kr, *Atmos. Environ., 23*, 25-35, 1989.

Y. J. Balkanski, Laboratoire de Modèlisation du Climat et de l'Environnement, CEA, Gif sur Yvette Cedex - 91191 France.

S. R. Beagley and J. de Grandpré, York University, 4700 Keele Street, Petrie Bldg, 153, North York, Ontario M3J 1P3 Canada.

D. J. Bergmann, J. E. Dignon, J. E. Penner, and D. A. Rotman, Lawrence Livermore National Laboratory, P.O. Box 808, Livermore, CA 94550.

W. T. Blackshear and W. L. Grose, NASA Langley Research Center, Hampton, VA 23681.

M. Brown, Aculight Corporation, 40 Lake Bellevue #100, Bellevue, WA 98005.

M. Chiba, Second Laboratory of Climate Research Devision, Meteorological Research Institute. 1-1, Nagamine, Tsukuba, Ibaraki, 305 Japan.

M. P. Chipperfield, K. Law, D. Z. Stockwell, and O. Wild, Department of Chemistry, University of Cambridge, Lensfield Road., Cambridge CB2 1EW England.

J. Feichter, Max-Planck-Institut für Meteorologie, Bundesstrasse. 55, D-20146 Hamburg, Germany.

C. Genthon, Laboratoire de Glaciologie et Géophysique de l'Environnement, CNRS, Domaine Universitaire BP 96, Saint Martin d'Hères, 38402, France.

D. J. Jacob, Division of Applied Sciences and Department of Earth & Planetary Sciences, Pierce Hall, 29 Oxford Street, Cambridge, MA 02138. (email: djj@io.harvard.edu)

P. S. Kasibhatla, School of Earth and Atmospheric Sciences, Georgia Institute of Technology, Atlanta, GA 30332.

I. Köhler, Institut für Physik der Atmosphäre, DLR Oberpfaffenhofen, D-82234 Wessling, Germany.

M. A. Kritz, Atmospheric Sciences Research Center, State University of New York at Albany, 1400 Washington Ave., Albany, New York, 12222.

M. J. Prather, Department of Geoscience, University of California at Irvine, Irvine, CA 92717.

M. Ramonet, Centre des Faibles Radioactivités, Laboratoire mixte CNRS/CEA, Gif sur Yvette Cedex, 91198 France.

P. J. Rasch, National Center for Atmospheric Research, Boulder, CO 80303.

C. E. Reeves, School of Environmental Sciences, University of East Anglia, Norwich NR4 7TJ, England.

R.-L. Shia, AER Inc., 840 Memorial Drive, Cambridge, MA 02139.

P. F. J. Velthoven and G. Verver, Royal Netherlands Meteorological Institute (KNMI), P.O.Box 201, 3730 AE De Bilt Netherlands.

H. Yang, Department of Applied Mathematics, University of Washington, Seattle, WA 98195.

P. Zimmermann, MOGUNTIA Global Modelling, Ludwigstrasse 10, D-65479 Raunheim, Germany.

(Received October 10, 1995; revised June 25, 1996;
accepted August 27, 1996.)